MIL-HDBK-1197
11 MARCH 1988

MILITARY HANDBOOK

AERO-ACOUSTICS TEST PROGRAMS

AMSC N/A

DISTRIBUTION STATEMENT A. APPROVED FOR PUBLIC RELEASE: DISTRIBUTION IS UNLIMITED

AREA FACR

ABSTRACT

This handbook provides basic design guidance on aircraft engine runup sound suppressors. It is intended for use by experienced architects and engineers and contains a review of model-scale and full-scale sound suppressed aircraft runup enclosure tests. The review provided the present checkout test data handbook.

Although it covers both model-scale and full-scale test data, it focuses on full-scale data with model-scale results included for comparison. The test data are presented in such a way as to make them readily applicable in a design situation.

FOREWORD

This military handbook has been developed from an evaluation of facilities in the shore establishment, from surveys of the availability of new materials and construction methods, and from selection of the best design practices of the Naval Facilities Engineering Command (NAVFACENGCOM), other Government agencies, and the private sector. It uses to the maximum extent feasible, national professional society, association, and institute standards. Deviations from this criteria, in the planning, engineering, design, and construction of Naval shore facilities cannot be made without prior approval of NAVFACENGCOMHQ Code 04.

Design cannot remain static any more than can the functions it serves or the technologies it uses. Accordingly, recommendations for improvement are encouraged and should be furnished to Naval Facilities Engineering Command, Southern Division, Code 406, P. O. Box 10068, Charleston, S.C. 29411-0068, telephone (803) 743-0458.

THIS HANDBOOK SHALL NOT BE USED AS A REFERENCE DOCUMENT FOR PROCUREMENT OF FACILITIES CONSTRUCTION. IT IS TO BE USED IN THE PURCHASE OF FACILITIES ENGINEERING STUDIES AND DESIGN (FINAL PLANS, SPECIFICATIONS, AND COST ESTIMATES). DO NOT REFERENCE IT IN MILITARY OR FEDERAL SPECIFICATIONS OR OTHER PROCUREMENT DOCUMENTS.

CONTENTS

CONTENTS

TABLES

FIGURES

FIGURES (Continued)

Section 1: INTRODUCTION

1.1 Background. Since 1973, the U. S. Navy has been involved in the aero-thermo and acoustic design of dry-cooled jet runup facilities. Initially, this involved only complete aircraft runup facilities (hush-house); but more recently engine test cells have been included. After construction, troubleshooting tests will be performed on a number of runup facilities as well as model-scale tests. The data from the model- and full-scale checkout tests constitute a significant source of design information. Consequently, this handbook was developed to summarize the results of all Navy runup facility tests. The tests can be subdivided as follows:

a) Full-scale tests:
   (1) post-construction facility checkout
   (2) diagnostic tests (troubleshooting)

b) Model-scale tests:
   (1) general (design) data
   (2) configuration verification

1.2 Full-Scale Test Emphasis. In this handbook the main emphasis is on full-scale test results with model-scale results presented for comparison. Table 1 contains a comprehensive definition of symbols pertinent to hush-house work.

Table 1
List of Symbols

A	Area - ft^2
A_A	Augmenter cross-sectional area
A_{door}	Hush-House door outlet flow area
$A_{encl\ eff}$	Enclosure effective flow area (A_{door} in hush-house case)
$A1_{net}$	House-House door inlet minimum flow area
$A2_{net}$	Hush-House secondary inlet minimum flow area
$A_{NT}(A_8)$	Engine nozzle throat area (total area at maximum power)
AIRCR	Aircraft
AUGM	Augmenter
Bar	Barometric pressure - inches of mercury absolute
Cp_{air}	Constant pressure specific heat of air - Btu/lb° F
Cp_E	Constant pressure specific heat of engine exhaust - Btu/lb° F
$Cp_{augm\ exh}$	Constant pressure specific heat of mixed flow leaving the augmenter - Btu/lb° F
D_{NT}	Engine nozzle throat diameter
E.P.R.	Exhaust nozzle pressure ratio($P_{T_{N(8)}}$/Bar)
g	Acceleration of gravity at sea level - 32.2 ft/sec^2
P	Static pressure - psi, inches of water, etc.
P_{encl}	Hush-House enclosure internal pressure
P_1	Static pressure at door inlet minimum area
P_2	Static pressure at secondary inlet minimum area
$P_{T_N}(P_{T_8})$	Exhaust nozzle total pressure
P_T	Stagnation pressure or total pressure
q	Dynamic pressure (1/2 ρV^2)
T or Temp	Temperature - ° F or ° R
T_{amb}	Ambient air temperature
T_p	Augmenter wall temperature parameter, $T_p = (T_{wall}-T_{amb})/(T_{T_N}-T_{amb})$ (dimensionless)
T_{wall}	Augmenter wall temperature
T_T	Stagnation temperature or total temperature
$T_{T_N}(T_{T_8})$	Engine nozzle exit total temperature
V	Velocity - ft/sec
V_{exit}	Augmenter exit velocity - ft/sec
V_{inlet}	Velocity at door inlet minimum area - ft/sec
$V_{interior}$ or V_{int}	Velocity approaching aircraft inside of hush-house
W	Mass flow rate - lbm/sec
W_{engine} or W_E	Total engine mass flow rate - lbm/sec
W_1	Door inlet mass flow rate - lbm/sec
W_2	Secondary inlet mass flow rate - lbm/sec
W_{IT}	Total inlet mass flow rate - lbm/sec
ρ	Air density - slugs/ft^3
Y_{ctr}	Lateral distance from augmenter centerline to augmenter wall - ft
Y_p	Lateral offset parameter, $Y_p=(Y_{ctr}-Y)/Y_{ctr}$ (dimensionless)

Section 2: DESCRIPTION OF TEST PROGRAMS

2.1 MIRAMAR #1 Hush-House. In 1973, a joint Navy-industry team was formed to determine the feasibility of developing a complete aircraft enclosure (hush-house) for the F-14A with a dry-cooled, sound suppressing exhaust system. The team reviewed available literature (refer to Aero-Thermal and Acoustical Data from the Postconstruction Checkout of the Miramar #2 El Toro Hush-House, J.L. Grunnet and I.L. Ver [1]) pertinent to dry-cooled exhaust systems and visited existing European dry-cooled hush-houses. Diagnostic tests on an F-4 semi-enclosure type of exhaust sound suppressor (refer to Observation of Fluidynamic Performance of Miramar NAS F-4, Acoustical Enclosure and Recommendations for Improvement, J.L. Grunnet [2]) and recommendations were a part of the team's initial responsibility. Modifications to the augmenter entrance, the waterspray pipes, the augmenter tube, and the perforated diffuser were recommended to improve pumping and reduce the recirculation of hot exhaust gases within the semi-enclosure. The design of the initial F-14A hush-house at NAS Miramar, California was then undertaken. Typical of most of the aircraft and engine runup enclosures that the team designed, the design was to meet the following criteria:

a) The facility must accept a variety of aircraft/engines.

b) The facility exhaust system is to be dry-cooled.

c) The engine inlet approach velocity shall be no greater than 50 f/s (15.24 m/s).

d) The maximum noise level around the aircraft/engine shall be no greater than 2 dBA above the corresponding noise during open field runup over a concrete pad or apron.

e) The exterior noise level shall be no greater than 85 dBA at 250 ft (76.2 m) from the engine nozzle exit, with one engine at maximum afterburner or two engines at military power.

f) The maximum exhaust system material temperature shall not exceed 800° F (427° C).

After the design of the first F-14A hush-house (Miramar No. 1) was complete, a 1/15 scale model test program was initiated to both verify the Miramar hush-house exhaust system design and provide general design information (refer to Aerodynamic and Acoustic Tests of a 1/15-Scale Model Dry-Cooled Jet Aircraft Quasar Noise Suppressions System, J.L. Grunnet and I.L. Ver [3]). The model included a properly scaled acoustical treatment. Tests were run at a model exhaust total temperature of 3000° F (1649° C) giving meaningful aero-thermo and acoustic data. The results indicated that the outdoor noise limit of 85 dBA at 250 ft from the nozzle exits would be met with one F-14 engine in maximum afterburner; however, even with an aligned aircraft, the augmenter wall temperature will reach 1000° F (538° C). These predictions were subsequently verified in the 1975 full-scale checkout of the Miramar No. 1 hush-house, according to this research. The higher than specified augmenter wall temperature necessitated a structural review of the augmenter design to verify that it can withstand local wall temperatures of 1000° F.

2.2 Miramar No. 2 and El Toro Hush-Houses. Next, designs for the second N.A.S. Miramar F-14 hush-house (Miramar No. 2) and an F-4, A-6 hush-house for MCAS El Toro, California were completed. The important changes between Miramar No. 1 and No. 2 included better faring of the door air inlet, a door outlet screen to reduce flow separation on the turning vanes, sound absorptive panels surrounding the augmenter inlet and nonperforated inconel panels in the hottest locations on the augmenter duct sidewalls. These facilities were checked out in 1978 and 1979, respectively, and the results were presented in Reference [1]. Prior to full-scale facility checkout, 1/11.4 scale model tests were run to verify that the A-6 exhaust can be captured by a 19 ft wide x 11 ft high augmenter entrance (refer to Aero and Thermodynamic Test of a 1/11.4-Scale Hush-House Augmenter Inlet, J.L. Grunner and J.H. Berger [10]).

2.3 NARF Norfolk Depot Test Cell Diagnostic Tests. TF-30P412/414 engines run up to maximum afterburning in the NARF Norfolk, Virginia depot cells 13 and 14 (refer to NARF-NORVA Test Cells 13 and 14 Diagnostic Tests and Recommendations, J.L. Grunnet [4]) gave an indication of excessive turbine station vibration while they would meet vibration limits in the older cells next door. Noise buildup in the reverberant cell enclosure was responsible for the high measured vibration level. Some improvement was obtained by moving the engine as far AFT as the mounting would allow, thus minimizing the axial distance between the engine nozzle exit and the augmenter throat and thereby reducing the cell interior noise level.

2.4 NATC Patuxent River Hush-House. Design of a hush-house type test and evaluation facility for NATC Patuxent, Maryland began in 1977. This facility had to accommodate the S-3A as well as the F-14A. In addition it had to provide a mist free environment with the aircraft enclosure and a maximum engine inlet approach velocity within the enclosure of only 30 f/s (9.1 m/s). These things necessitated the incorporation of a secondary air inlet located above the augmenter entrance. Model tests were run to verify acceptable flow capture with the S-3A (refer to 1/15-Scale Cold-Flow Model Tests of the Patuxent River Hush-House Configuration, J.L. Grunnet [11]) and to check augmentation and "cell" depression. Adequate performance was indicated. In 1983, after completion of the facility a complete full-scale checkout was run (Refer to Aero-Thermo and Acoustical Data from the Postconstruction Checkout of a Hush-House Located at NATC Patuxent River, MD, J.L. Grunnett [9]).

2.5 Test Cell Emissions Study. For a number of years the Navy has been striving to meet local district restrictions on test cell and hush-house exhaust plume opacity. In 1980, this culminated in a study of factors effecting exhaust plume opacity. The study included both full-scale observations and model-scale tests. A number of guidelines for exhaust system design were derived for minimizing plume opacity (refer to Phase I Report - The Effect of Test Cell Exhaust System Design on Exhaust Plume Opacity- Analysis and Observations and Phase II and III Report - The Effect of Test Cell Exhaust System Design on Exhaust Plume Opacity--Model-Scale Plume Opacity Tests and Design Procedures to Minimize Opacity, J.L. Grunnet and W.H. Phillips [5,12].

2.6 Miramar Hush-House Augmenter Failure Study. Long term operation of the Miramar Numbers 1 and 2 hush-houses began to produce structural failures in the augmenter sidewalls near the upstream end. This was believed to be due to high wall temperatures during operation of misaligned F-14A aircraft in maximum afterburner. Full-scale F-14A tests were run with various degrees of lateral misalignment (refer to A Study of Structural Failures in the Hush-Houses at NAS Miramar, J.L. Grunnet and G. Getter [6]). The maximum augmenter wall temperatures were indeed sensitive to misalignment. Suggested ways of reducing the structural damage included:

a) better F-14A alignment
b) fiberglass pillows more tightly packed
c) better placement of the unperforated Inconel augmenter face sheets
d) application of stress relief slots in certain augmenter section aft bulkheads.

Methods of reducing the maximum augmenter wall temperature through application of an augmenter inlet forcing cone or flare were checked at model-scale during 1983 (refer to 1/15 Scale Model Tests of a Forcing Cone Augmenter Pickup for Hush-Houses and Test Cells and Holt Flow Model Tests of a 1/15 Scale Hush-House with Augmenter Flare and Forcing Cone Flow Pickups, both by T.F. Buckley and T.J. McDonald [14, 15]). An augmenter flare, such as incorporated in the Patuxent River augmenter, resulted in significantly lower wall temperatures. During the Patuxent River hush-house checkout, both engines of the F-14 were run up to maximum afterburning thrust without damage to the exhaust system.

2.7 MCAS Cherry Point Pegasus Demountable Cell Tests. In 1982, diagnostic tests of the F402 Pegasus engine in the A/E 32T-15 engine test enclosure (demountable test cell) were performed at MCAS Cherry Point, North Carolina (refer to Aerodynamic Measurements Mode in the Marine A/E 32T-15 Engine Test Enclosure at Cherry Point (F-402-2), Relative to Pegasus Acceleration Lay and Subsequent Conclusions and Recommendations, J.L. Grunnet [7]). An apparent engine acceleration lag was being encountered such that acceleration time specs could not always be met. Checks were made of the fuel system, cell enclosure flow field etc, and it was concluded that the fan inlet distortion was larger than desirable. It was finally discovered that a tachometer circuitry problem was responsible for the indicated lag, but changes to improve the cell flow were recommended anyway.

2.8 AV-8 Harrier Hush-House Model Tests. In 1982, a 1/15 scale model of a Harrier hush-house was tested to verify adequate flow pickup and to determine augmenter pumping (refer to 1/15-Scale Cold-Flow Model Tests of a Hush-House with Simulated AV-8 Aircraft Exhaust, J.H. Berger and J.L. Leuck [13]). Reasonably good flow pickup was demonstrated over the whole range of nozzle vector angles from 0° F to 98° F (-18° C to 37° C). Augmentation ratio remained relatively constant at 3.5 over the entire range of nozzle vector angles. Since the date of the model tests a full-scale Harrier hush-house design has been completed.

2.9 NAS Dallas Test Cell. In 1979, a jet engine test cell was designed for N.A.S. Dallas incorporating the dry-cooled sound absorptive augmenter exhaust system concept. This was checked out in 1983 (refer to Aero-Thermo Checkout of NAS Dallas Dry-Cooled Jet Engine Test Cell, J.L. Grunnet and N.C. Helm [8]). External noise limits were exceeded and this has resulted in consideration of alternative augmenter inlet designs which avoid noise generation.

Results of most checkout and model tests run to date were summarized in Model Test and Full-Scale Checkout of Dry-Cooled Jet Runup Sound Suppressers, J.L. Grunnet and E. Ference [16]. This reference contains additional historical background and more detail regarding hush-house sound supression.

Section 3: AIRCRAFT AND ENGINE DATA

3.1 Aircraft Propulsion Systems and Geometrical Data. The hush-houses built to date accommodate a wide range of aircraft types. Information regarding each aircraft to be accommodated is essential in the design of the enclosure and its exhaust system. Table 2 relates each aircraft type to its propulsion system characteristics. This information is essential in establishing total enclosure and inlet flow rates as well as maximum exhaust temperatures. Table 3 presents important aircraft geometrical information related to hush-house and augmenter pickup sizing. In every case the engine exhaust plane must be at least 4 ft (1.22 m) forward of the augmenter inlet.

Table No. 2
Aircraft Engine Data

Aircraft	No. of Engines	Engine Type	Flow Rate WE pps	EPR	Power Setting	Temp. T_{TN} °R	Throat Area ANT sq ft	Thrust lb
A-4	1	J-52P408	140	3.3	Mil	1880	1.89	11,000
A-6	2	J-52P8	140	2.7	Mil	1640	1.91	9,000
A-7	1	TF-41A						
			260	2.5	Mil	1540	3.38	15,000
AV-8B	1	F-402RR406						
			460	2.2	Mil	1300 Avg.	Total 6.59	24,000
F-4	2	J-79GE8 or 10	170	2.5	Mil	1600	2.52	11,000
					A/B	3500	4.20	17,000
F-5	2	J-85GE21	53	2.5	Mil	1600	0.76	3,500
					A/B	3600	1.25	5,000
F-8	1	J-57P420	180	2.6	Mil	1684	2.77	11,000
					A/B	3500	4.62	19,000
F-14A	2	TF-30P412/414	245	2.1	Mil	1400	3.56	12,000
					A/B	3600	7.50	20,000
F-18	2	F-404GE	140	3+	Mil	1600	1.76	10,000
					A/B	3600	2.88	16,000
S-3	2	TF-34GE	343	1.6	Mil	1000 Avg.	Total 6.02	10,000
T-2A	1	J-34(Westinghouse)	62	2.2	Mil	2100	1.29	3,400
T-2C	2	J-85GE4	44	2.5	Mil	2000	0.69	3,500

Table 3
Aircraft and Enclosure Geometry Data

Aircraft	b_{ft}	l_{ft}	$X_{N_{ft}}$	Y_{ft}	Z_{ft}	a_s	a_v
A-4	27.5	40	14	---	7.0	---	- 5.5
A-6	53	55	27	3.5	5.0	6.0	-12.0
A-7	39	46	8	---	6.0	---	- 4.0
AV-8B	30	46	30	2.6	5.0	5.0	- 9.0(fan)
F-4	38.5	58	15	2.3	6.5	0	- 4.5
F-5	26.5	48	5	0.9	5.2	-1.5	0
F-8	35	54	4	---	5.3	---	- 4.0
F-14A	64	62	5	4.5	6.3	1.0	1.3
F-18	37.5	56	3.5	1.4	4.5	0	0
S-3	68.5	53	33(fan)	7.8	5.0	0	1.5
T-2A	38	38	22	---	3.6	---	- 4.0
T-2C	38	38	22	1.0	3.5	0	- 4.0

b = Wing span (extended).
l = Aircraft length.
X_N = Distance from engine nozzle exit to enclosure aft wall.
Y = Lateral distance from aircraft centerline to engine nozzle exit centerline.
Z = Vertical distance from floor to engine nozzle centerline with centerline leveled.
a_s = Lateral jet centerline deflection - positive outward.
a_v = Vertical jet centerline deflection (unleveled) - positive upward.

Section 4: HUSH-HOUSE AND TEST CELL GEOMETRICAL DATA AND INSTRUMENTATION DEFINITION

4.1 Hush-House Geometrical Data. Table 4 contains tabular geometrical information for all of the existing Navy hush-houses. Figures 1 (Miramar), 2 (El Toro), 3 and 4 (Patuxent River) and 5 (Dallas) include dimensioned plan and side elevation views of the existing Navy dry-cooled runup facilities. The geometrical information on Table 4 includes inlet net areas, augmenter duct area, etc., as well as linear dimensions. Figures 1, 2, 4 and 5 also show the location of permanent pressure and temperature instrumentation provided with each facility. P_{encl} data are taken during engine trim runs. The augmenter wall temperatures indicate overtemperature during normal runs. All of this instrumentation was used during the facility checkouts, reported herein.

4.2 Pressure/Temperature Instrumentation. For postconstruction facility checkout, additional instrumentation was provided to measure air inlet static pressures (reduced to inlet mass flow rate), enclosure interior dynamic pressure (reduced to enclosure velocity), and augmenter exit total pressures and temperatures (reduced to augmenter exit velocity). Figure 3 shows the location of augmenter exit rakes used during the Miramar No. 2 and El Toro checkouts.

4.3 Postconstruction Noise Data Collection. Extensive noise data were also taken during postconstruction facilities checkouts. Microphones were located externally at 30° intervals on a 250 ft (76.2 m) radius circle centered on the engine exhaust plane location. In addition, there was usually one microphone located at 1000 ft (304.8 m) from the engine exhaust plane. Microphones were also placed inside the aircraft or engine enclosure alongside the aircraft or engine and data taken that could be compared with the free field measurements. Noise data are discussed in Sections 11 and 12.

Table 4
Hush-House and Test Cell Geometrical Information

Facility	Primary Inlet				Secondary Inlet		Enclosure		Augmenter			
	Length ft	Net Area ft^2	Effec. Area ft^2	Outlet Area ft^2	Net Area ft^2	Effec. Area ft^2	Width ft	Length ft	Pickup Width ft	Basic Width ft	A_A ft^2	L_A* ft
Miramar #1	67	335	285	738	---	---	78	72	19	19	183	90
Miramar #2	67	335	300	738	---	---	78	72	19	19	183	90
El Toro	57	285	230	627	---	---	68	64	19	14	109	67
Patuxent River	70	350	315	770	140	126	85	80	23	19	183	95
Dallas (Test Cell)	--	185	170	500	---	---	25	57	8.67	11.5	104	60

*L_A = Distance from aircraft enclosure aft wall to augmenter exit

Aircraft and Engine Handling Capability to Each Hush-House

Miramar #1	A-4*, A-6, A-7, F-4*, F-5 (T-38), F-8*, F-14*, F-18
Miramar #2	A-4, A-6, A-7, F-4*, F-5, F-8, F-14*, F-18
El Toro	A-4*, A-6*, F-4*, Bare J-79*
Patuxent River	A-4, A-6*, A-7, F-4*, F-5, F-8, F-14*, F-18, S-3*, T-2A, T-26
Dallas Test Cell	J-79*, TF-41

*Test Data Available

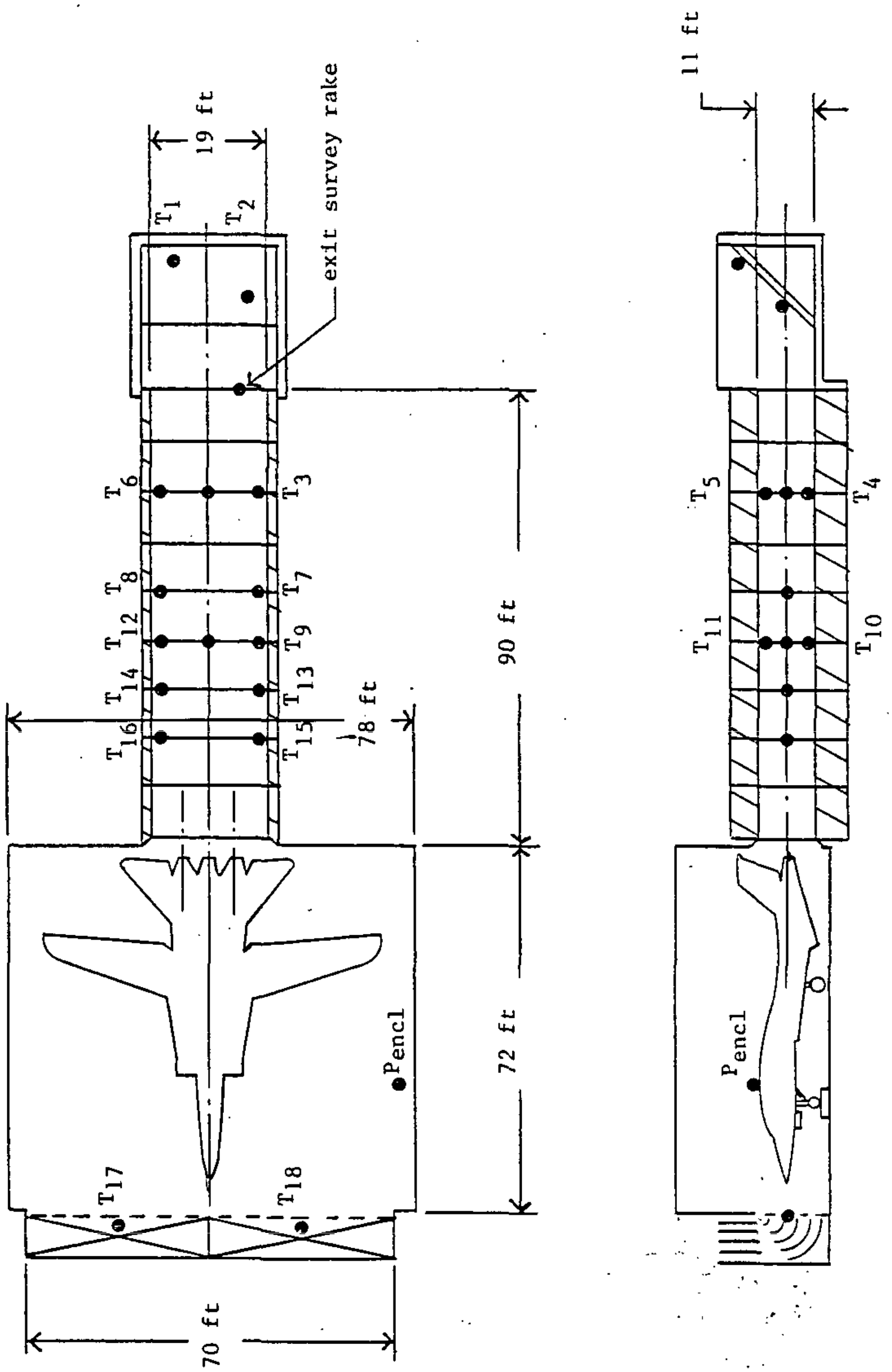

Figure 1
Miramar Layout Showing Thermocouple Locations

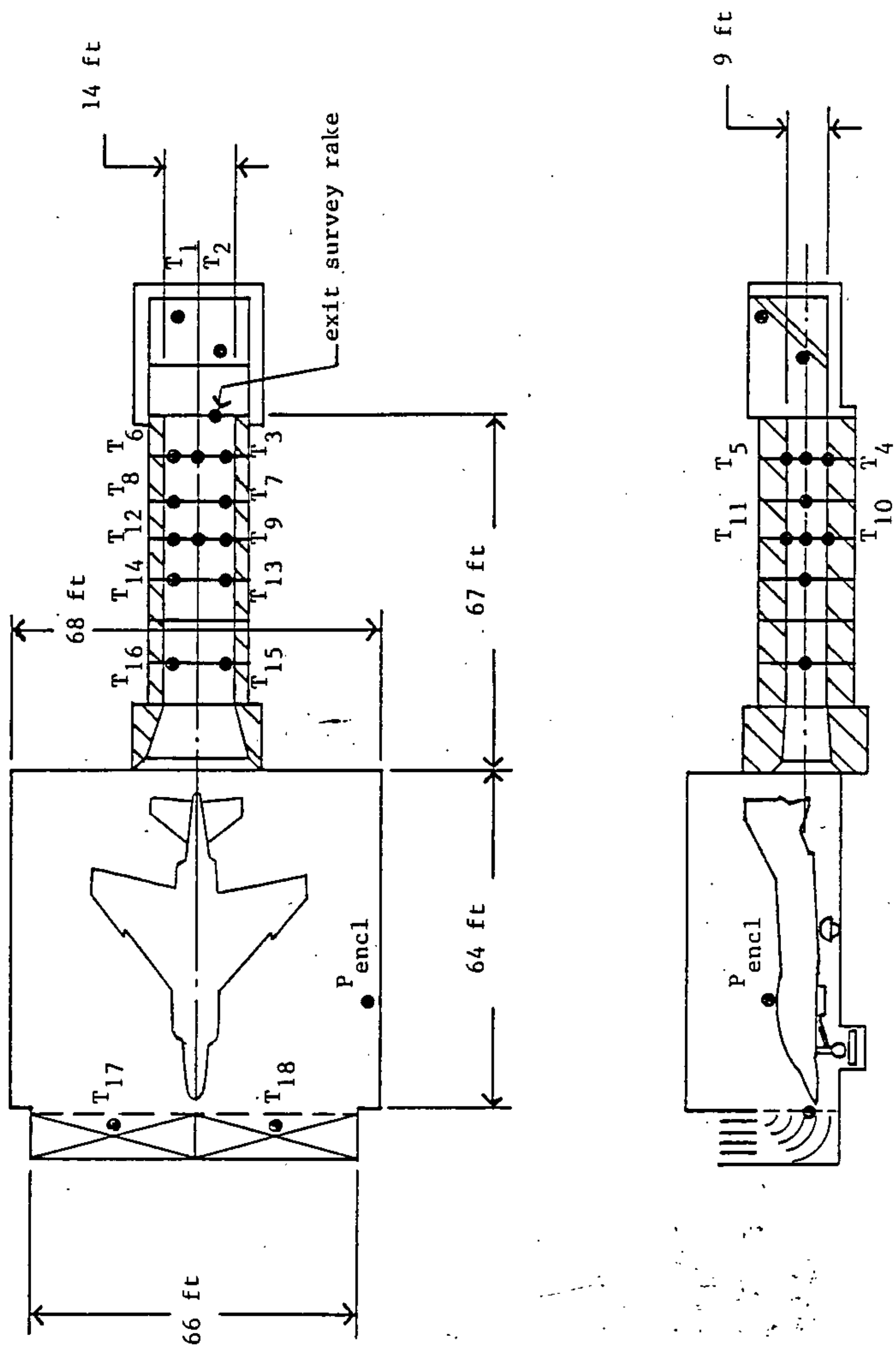

Figure 2
El Toro Layout Showing Thermocouple Locations

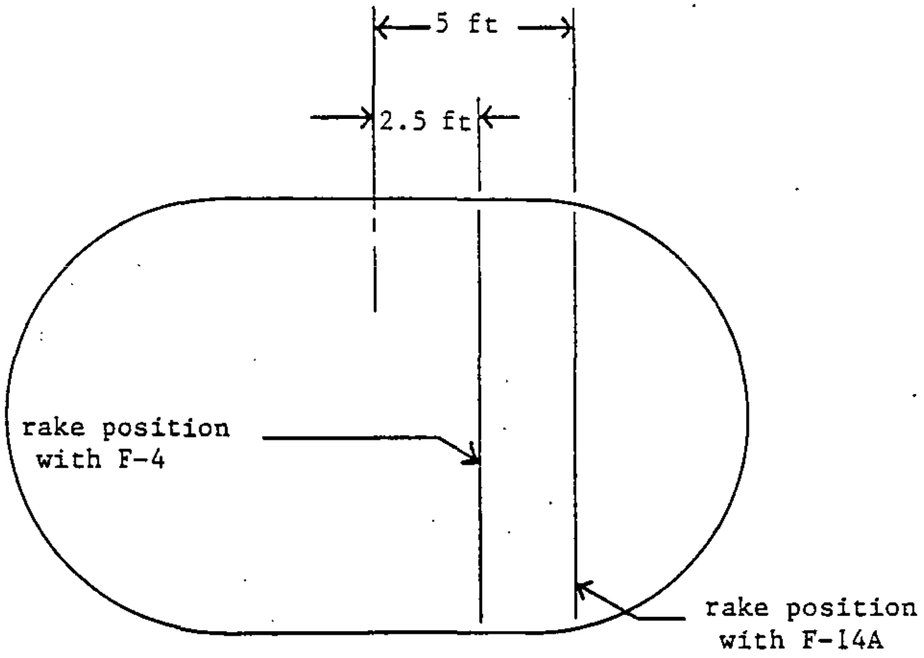

A. Miramar No. 2

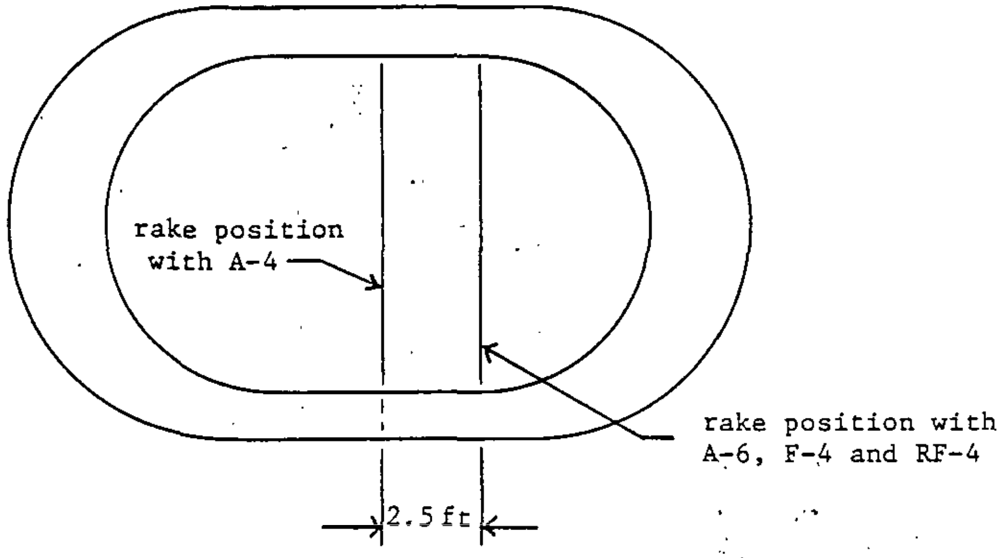

B. El Toro

Figure 3
Miramar No. 2 and El Toro Augmenter
Cross-Sections Showing Rake Locations

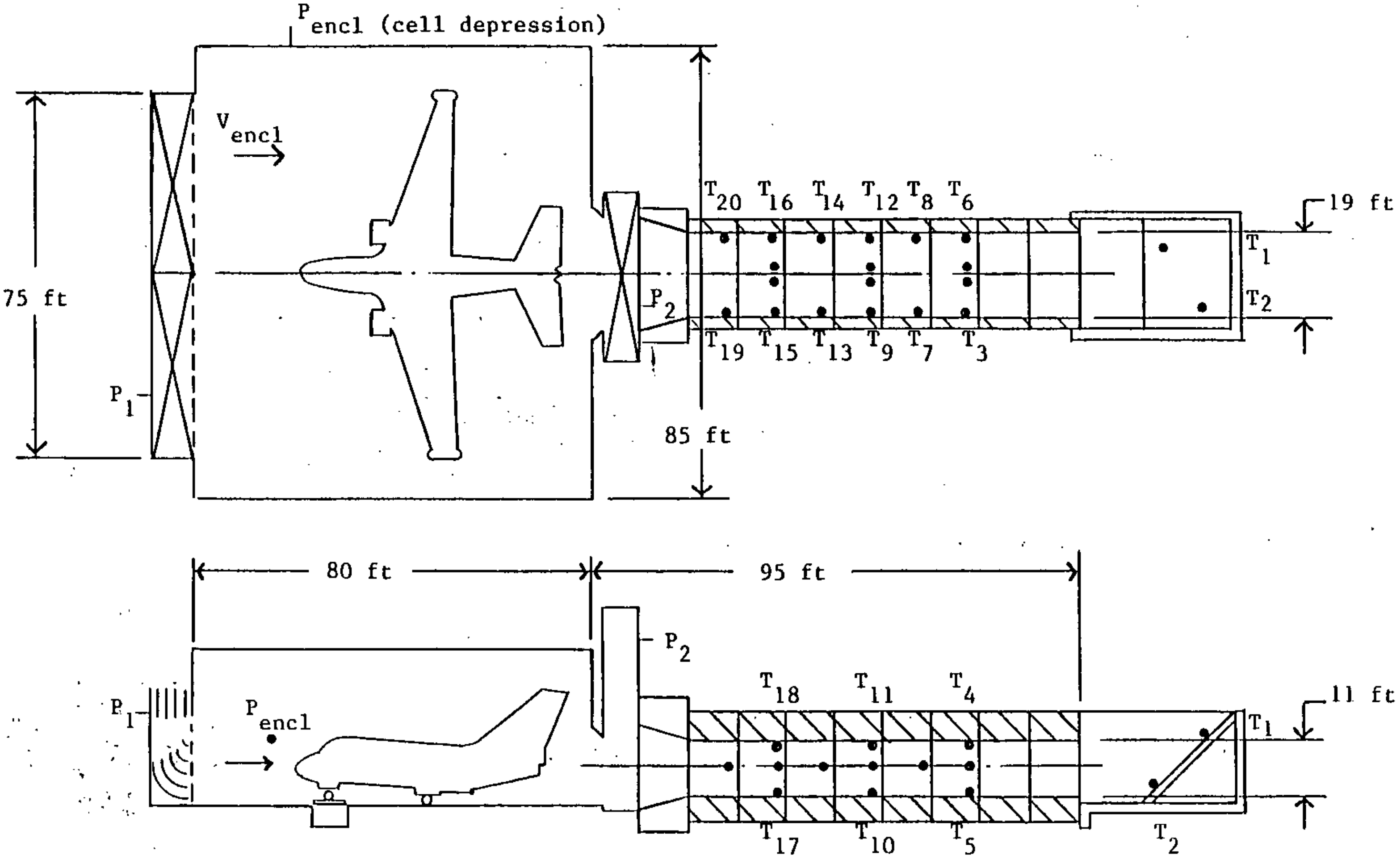

Figure 4
Patuxent River Layout Showing Thermocouple Locations

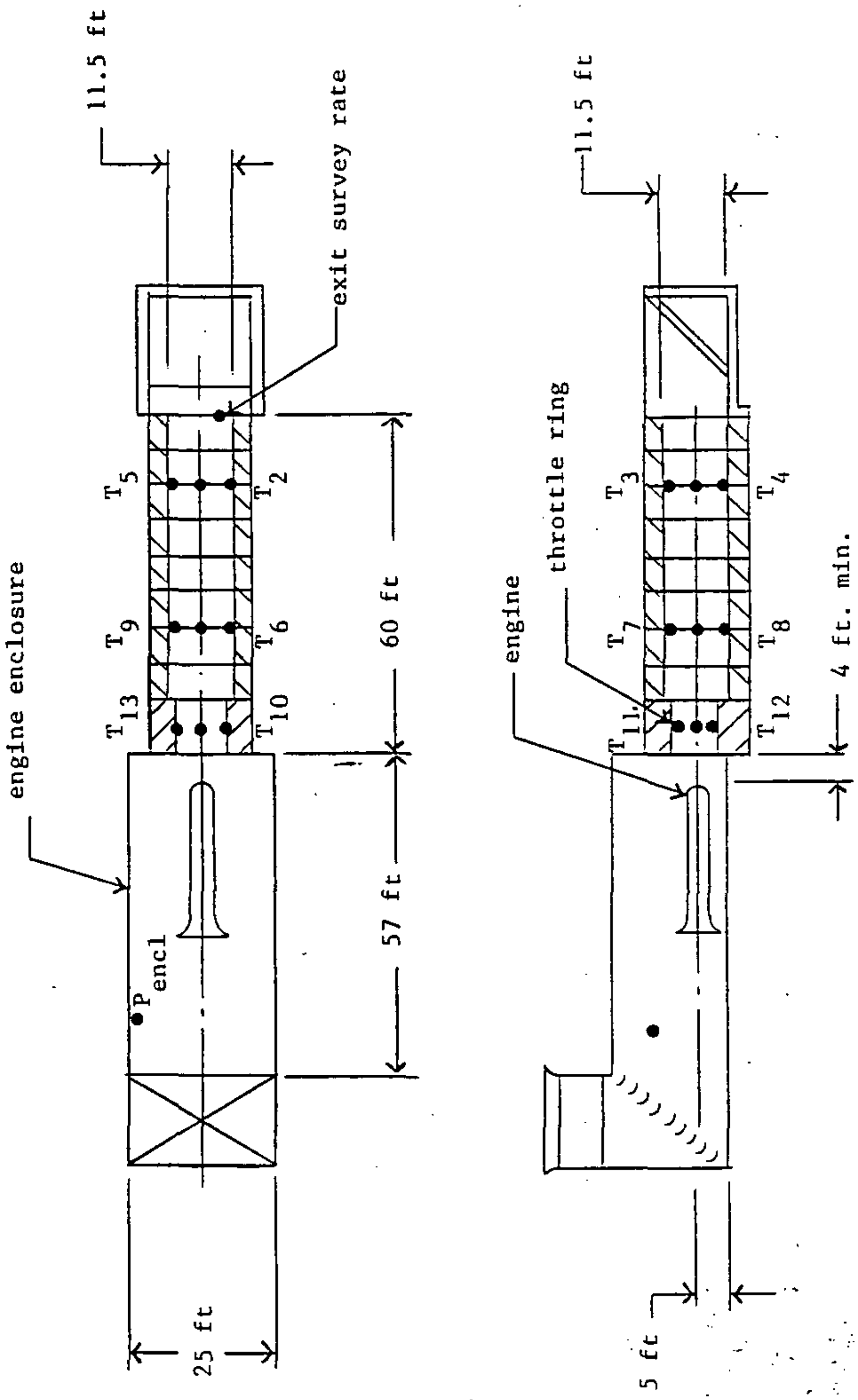

Figure 5
Dallas Layout Showing Thermocouple Locations

Section 5: CHECKOUT DATA SUMMARY

5.1 Postconstruction Facility Checkout Data. Table 5 contains the basic test information obtained from each of the postconstruction facility checkouts. This includes primary inlet, secondary inlet, and total inlet air mass flow rates for each aircraft and engine thrust setting, as well as the corresponding enclosure interior velocity, "cell" depression and maximum augmenter wall, and ramp surface temperatures. The information is arranged chronologically in the order in which the facilities were checked out.

Table 5
Basic Checkout Data with Aligned Aircraft

Facility	Aircraft	Thrust Setting	Primary Inlet Flow $\dot{W}_1$ pps	Secondary Inlet Flow $\dot{W}_2$ pps	Total Inlet Flow $\dot{W}_{IT}$ pps	Enclosure Int. Press "H_2O"	Enclosure Velocity fps	Max T_{Aug} °F	Max T_{Ramp} °F
Miramar No. 1	A-4	(1) Mil	1615	–	1615	-0.75	47	149	162
	F-4	(1) Mil	1568	–	1568	-0.75		201	195
	F-4	(1) A/B	1615	–	1615	-0.80	49	471	420
	F-4	(2) Mil	2280	–	2280	-1.40	58	215	237
	F-8	(1) Mil	1615	–	1615	-0.70	46	164	168
	F-8	(1) A/B	1710	–	1710	-0.80	49	394	373
	F-14A	(1) Mil	1686	–	1686	-0.85	46	215	204
	F-14A	(1) A/B	1615	–	1615	-0.90	49	970	660
	F-14A	(2) Mil	2470	–	2470	-1.75	68	–	202
Miramar No. 2	F-4	(1) Mil	1700	–	1700	-0.70	24	186	192
	F-4	(2) Mil	2220	–	2220	-1.15	31	217	234
	F-4	(1) A/B	1700	–	1700	-0.70	24	436	447
	F-14A	(1) Mil	1450	–	1450	-0.60	24	203	200
	F-14A	(2) Mil	2530	–	2530	-1.50	37	215	206
	F-14A	(1) A/B	1450	–	1450	-0.60	24	990	674
El Toro	A-4	(1) Mil	1550	–	1550	-1.10	31	192	187
	A-6	(1) Mil	1020	–	1020	-0.50	23	256	212
	A-6	(2) Mil	1360	–	1360	-0.90	28	303	243
	F-4	(1) Mil	1310	–	1310	-0.80	26	209	189
	F-4	(2) Mil	1730	–	1730	-1.30	34	256	236
	F-4	(1) A/B	1310	–	1310	-0.80	26	470	440

Table 5 (Continued)
Basic Checkout Data with Aligned Aircraft

Facility	Aircraft	Thrust Setting	Primary Inlet Flow $\dot{W}_1$ pps	Secondary Inlet Flow $\dot{W}_2$ pps	Total Inlet Flow $\dot{W}_{IT}$ pps	Enclosure Int. Press "H_2O"	Enclosure Velocity fps	Max T_{Aug} ° F	Max T_{Ramp} ° F
Patuxent River	A-6	(1) Mil	1150	490	1640	-0.75	13	220	175
	A-6	(2) Mil	1420	490	1910	-1.46	19	221	206
	F-4	(1) Mil	1280	850	2130	-0.76	14	197	188
	F-4	(2) Mil	1460	1090	2250	-1.16	19	230	234
	F-4	(1) A/B	1280	830	2110	-0.76	14	400	351
	F-4	(2) A/B	-	-	-	-	-	-	-
	F-14A	(1) Mil	1080	830	1910	-0.76	15	202	194
	F-14A	(2) Mil	1430	1220	2650	-1.35	22	186	191
	F-14A	(1) A/B	1030	750	1780	-0.60	10	619	441
	F-14A	(2) A/B	1305	930	2235	-1.12	19	757	554
	S-3A	(1) Mil	1260	240	1500	-1.03	19	124	116
	S-3A	(2) Mil	1900	0	1900	-2.35	30	132	128
NAS Dallas*	Bare J-79	(1) Mil	1250	-	1250	-0.80	25	225	-
(Throttle ring in)	Bare J-79	(1) A/B	1250	-	1250	-0.80	25	615	-
NAS Dallas*	Bare J-79	(1) Mil	1600	-	1600	-1.07	34	190	-
(Throttle ring out)	Bare J-79	(1) A/B	1600	-	1600	-1.07	34	510	-

*Note: Enclosure internal pressure and velocity data for zero cross wind.

Section 6: AUGMENTER MASS FLOW RATE

6.1 Augmenter Mass Flow Correlations. Figures 6, 7 and 8 contain the augmenter mass flow (pumping) correlation based upon all of the postconstruction facility checkout data. In this correlation, the total inlet air mass flow to engine flow rate ratio is plotted versus the ratio of augmenter duct area to engine flow rate. This form of correlation suggested itself after the first Miramar checkout where it was noted that total inlet flow rate remained constant during excursions from military thrust to maximum afterburning thrust (engine mass flow rate remaining constant). This form of correlation is fairly accurate as long as the augmenter duct area, A_A, is larger than the engine nozzle throat area ($A_A > 10A_{NT(8)}$) and the total pressure rise in the pumped flow is lower than the engine nozzle total pressure (P_{TFlow} $0.005\ P_{TN(8)}$). Augmenter pumping then becomes primarily the functions of relative augmenter duct area (increased pumping with increased duct area) and the location and orientation of the exhaust nozzle centerlines with respect to the augmenter duct boundaries (maximum pumping with engine exhaust centered and aligned in augmenter).

6.1.1 Exhaust Data from Augmenter Center. Figure 6 presents data for aircraft/engine situations where the engine exhaust was centered in the augmenter. Model test results are included for reference. These data represent the maximum pumping performance with an essentially constant area augmenter duct. Model test data reported in [3] show that significant increases in pumping can be obtained by incorporating a subsonic diffuser on the augmenter. For the facilities covered herein, however, the constant section augmenter duct provided adequate pumping of cooling air and the constant section duct is less expensive to build. Moreover, increasing total air flow above the minimum needed for cooling can require a bigger, more costly, air inlet. In the case of the NAS Dallas test cell, a throat section was included at the upstream end to limit pumping to only cooling. This made it possible to reduce the air inlet net area and to limit the cell velocity to less than 50 f/s (15.2 m/s) without a secondary air inlet.

6.1.2 Correlation for Bare J-79 Engines and F-79 Powered F-14. Figure 7 contains the augmenter mass flow correlation for bare J-79 engines and the J-79 powered F-4. This correlation involves centered and nearly-centered and aligned engines. Thus, the pumping is close to maximum. In Figure 7 the effect of a throttle ring (in addition to the throat) in the N.A.S. Dallas test cell is shown.

6.1.3 Effect of Engine Centerline Offset. Figure 8 shows the effect of significant engine centerline offset and misalignment on augmenter pumping. In the case of the F-14, the nozzle centerlines are 9 ft (2.74 m) apart and splayed outward 1° with an augmenter of 19 ft (5.79 m) width. The exhaust centerlines for the S-3A are 16 ft (4.88 m) apart and necessitate an enlarged flow pickup upstream of the 19 ft wide augmenter duct. Figure 8 contains model test data from Reference [11] for comparison.

6.1.4 Augmenter Length Selection. The augmenter length for the various dry-cooled facilities was chosen in every case on the basis of required noise suppression, since the augmenter with its absorptive liner is an important exterior noise reduction component. Pumping data suggest that adequate

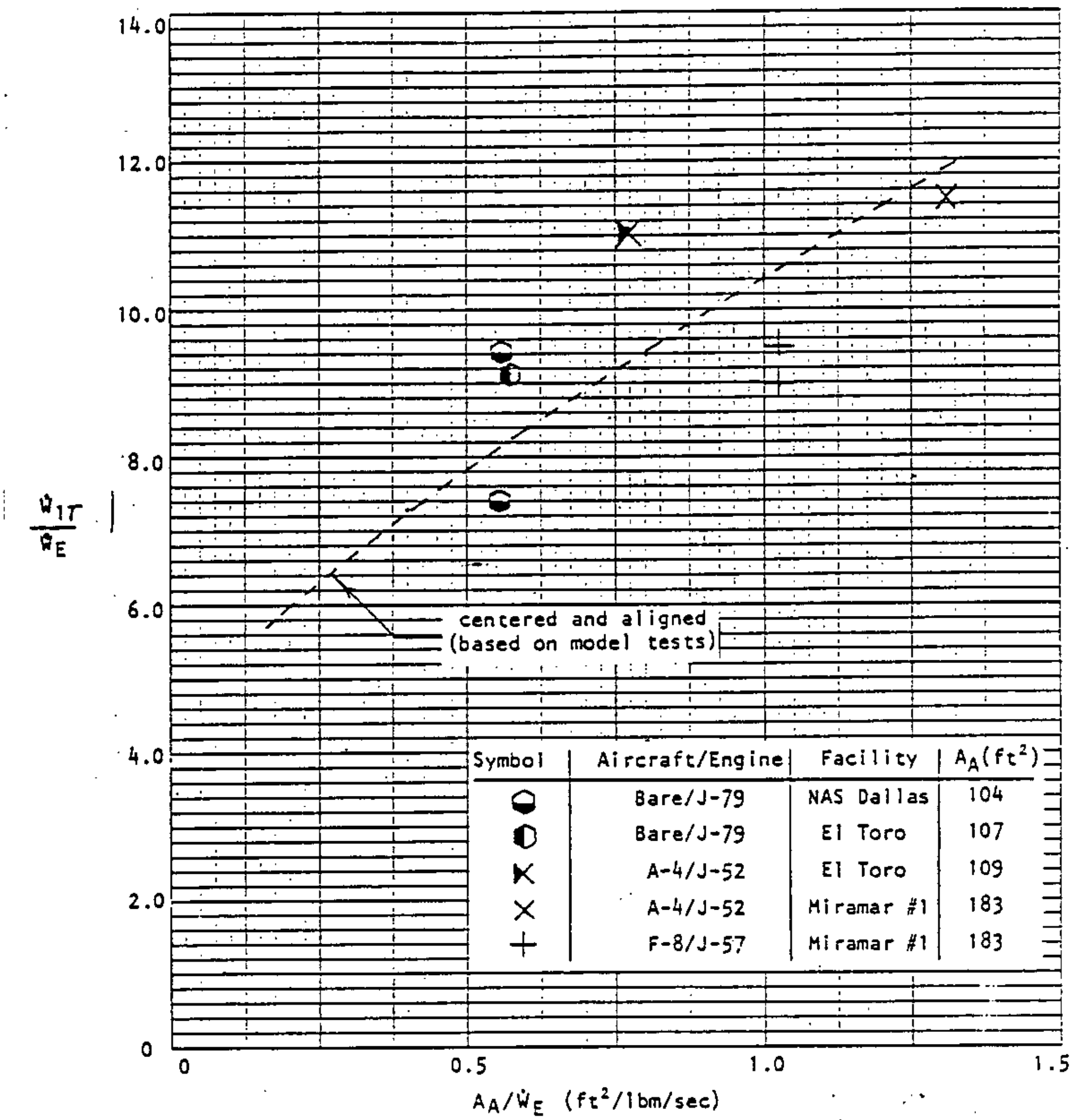

Figure 6
Augmenter Mass Flow Correlation with
Engine Centered and Aligned

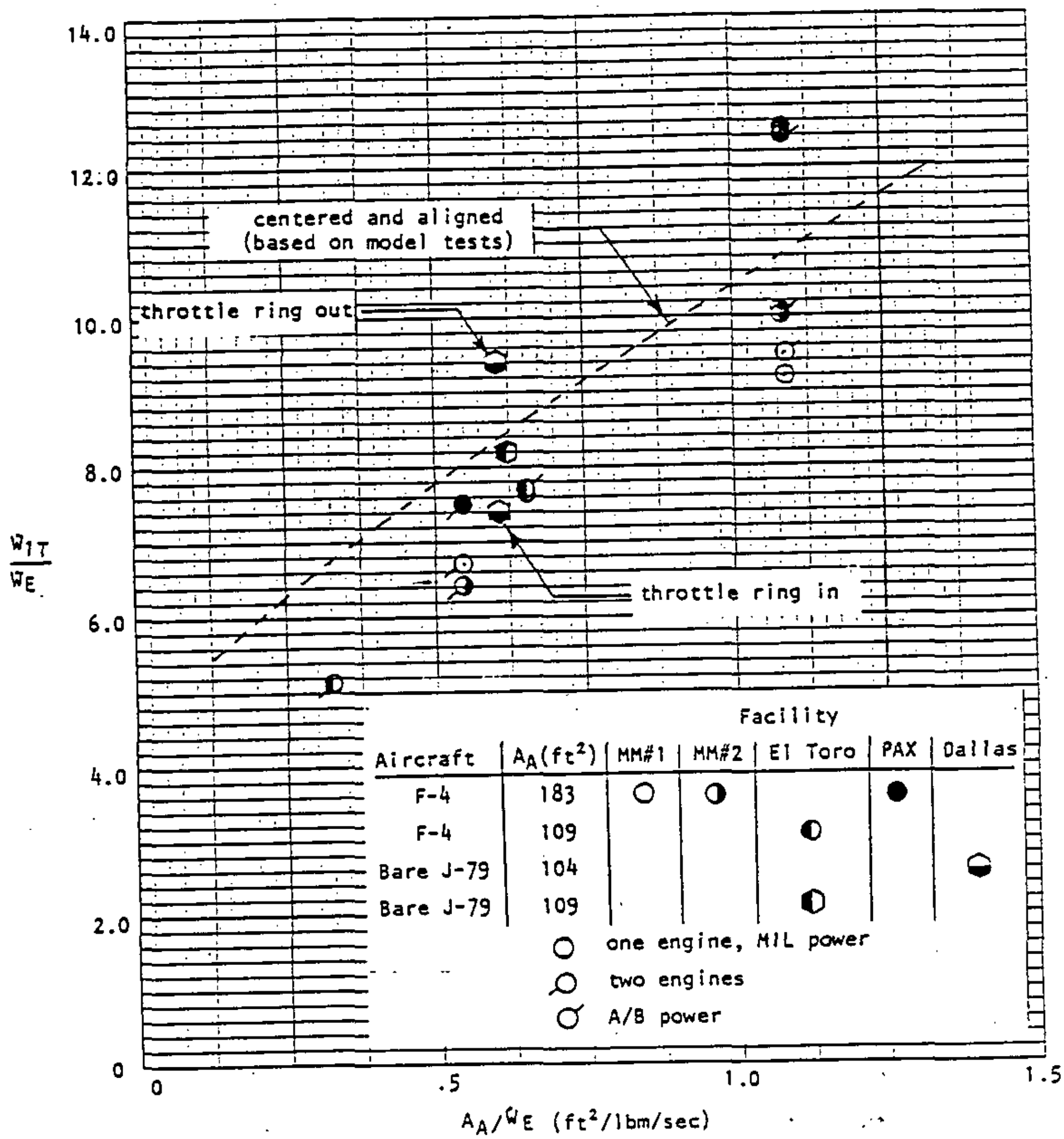

Figure 7
Augmenter Mass Flow Correlation
for J-79 Engine and J-79 Powered F-4

Aircraft	α_s	Y_D	A_A	Facility MM#1	Facility MM#2	Facility El Toro	Facility PAX
F-14A	1°	.47	183	△	◭		▲
S-3A	0°	.82	183				◆
A-6	6°	.37	183				●
A-6	6°	.51	109			◧	

○ one engine, MIL power
ọ two engines
ơ A/B power

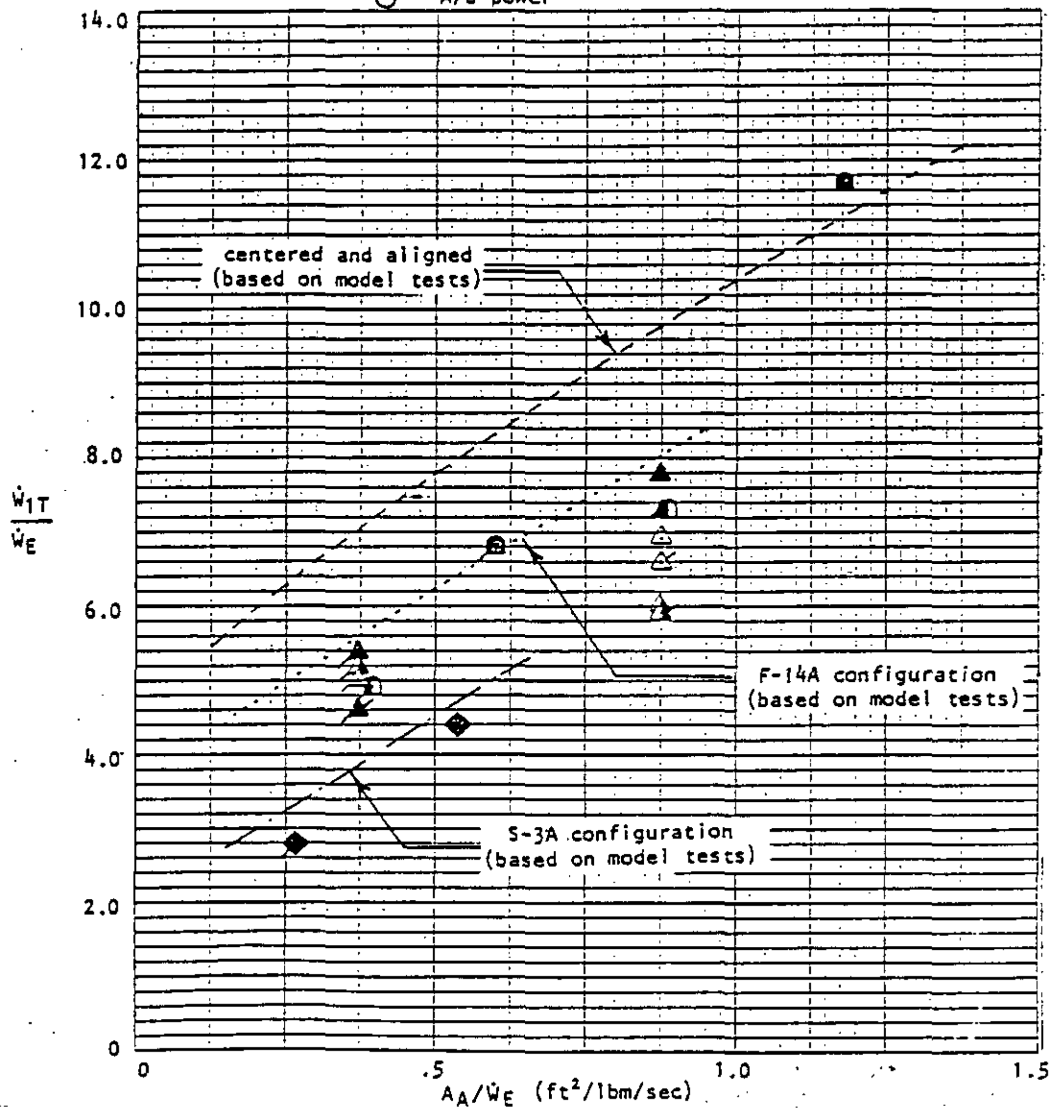

Figure 8
Augmenter Mass Flow Correlation with
Significant Engine Centerline Offset
and Misalignment

pumping of cooling air can be obtained with an augmenter 3 to 4 effective diameters long, or about 2/3 the chosen length [3]. The relative insensitivity of pumping to augmenter length is related to the low-pumped flow pressure rise required.

Section 7: ENCLOSURE INTERIOR FLOW CONDITIONS

7.1 Enclosure Interior Conditions. Enclosure interior conditions of interest include:

a) interior pressure (cell depression)
b) velocity approaching aircraft/engine inside of enclosure - V_{int}
c) enclosure interior flow patterns

hush-house/test cell designs are based on providing acceptable interior conditions from the standpoint of the enclosure structure, engine operation and personnel comfort and safety. Thus, it is typical to limit cell depression to 2 in. (50.76 mm) H_2O, interior velocity to 50 f/s (15.24 m), and to avoid significant recirculation of exhaust gases within the enclosure.

7.1.1 Interior Pressure. Interior pressure (cell depression) data are presented in Table 5 and in Figures 9 and 10. It is apparent from a comparison of Figures 9 and 10 that hush-house cell depression data group best when plotted versus the specific flow rate through the primary between-the-baffles net area ($\dot{W}_1/A_{1net}$). The Patuxent River hush-house primary exhibits a higher loss because of the inclusion of demisting elements. The N.A.S. Dallas test cell exhibits lower loss because the vaned turn from vertical to horizontal does not involve flow deceleration. Note that the cell depression varies roughly as the square of the specific flow rate or, i.e., as the dynamic pressure in the minimum net area A_{1net}.

7.1.2 Interior Velocity. Table 5 and Figures 11, 12 and 13 present enclosure interior velocity, V_{int} data. A comparison between Figures 11, 12 and 13 indicates that the best correlation occurs with specific mass flow rate based upon the effective flow area within the enclosure. (A_{door} in the case of a hush-house and total cell cross-section in the case of the N.A.S. Dallas test cell.) The velocity measurements used in Figures 11 through 13 were taken 15 ft (4.57 m) from the hush-house door outlet and about 10 ft (3.05 m) into the constant height test cell in the case of N.A.S. Dallas.

7.1.3 Interior Flow Patterns. Enclosure flow patterns are of interest because of concerns about exhaust recirculation in the hush-houses and, in the case of the A/E 32T-15 Pegasus dedicated test cell at MCAS Cherry Point, concerns about bad compressor face distortion arising from ingestion of low energy flow. Figures 14 and 15 show enclosure interior flow patterns with the A-6 at El Toro and with the S-3A at Patuxent River respectively. The A-6 and S-3A represent the most difficult hush-house flow capture problem. In both cases, the degree of recirculation appears to be acceptable (in the case of the S-3A, this is true because most of the recirculation involves relatively cool air from the fan exhaust). Figure 16 shows A/E 32-T15 interior flow patterns during F-402 Pegasus runup. A recommendation was made that the cell flow rate be increased to minimize low energy air ingestion, even though the problem being addressed did not result from the flow distribution.

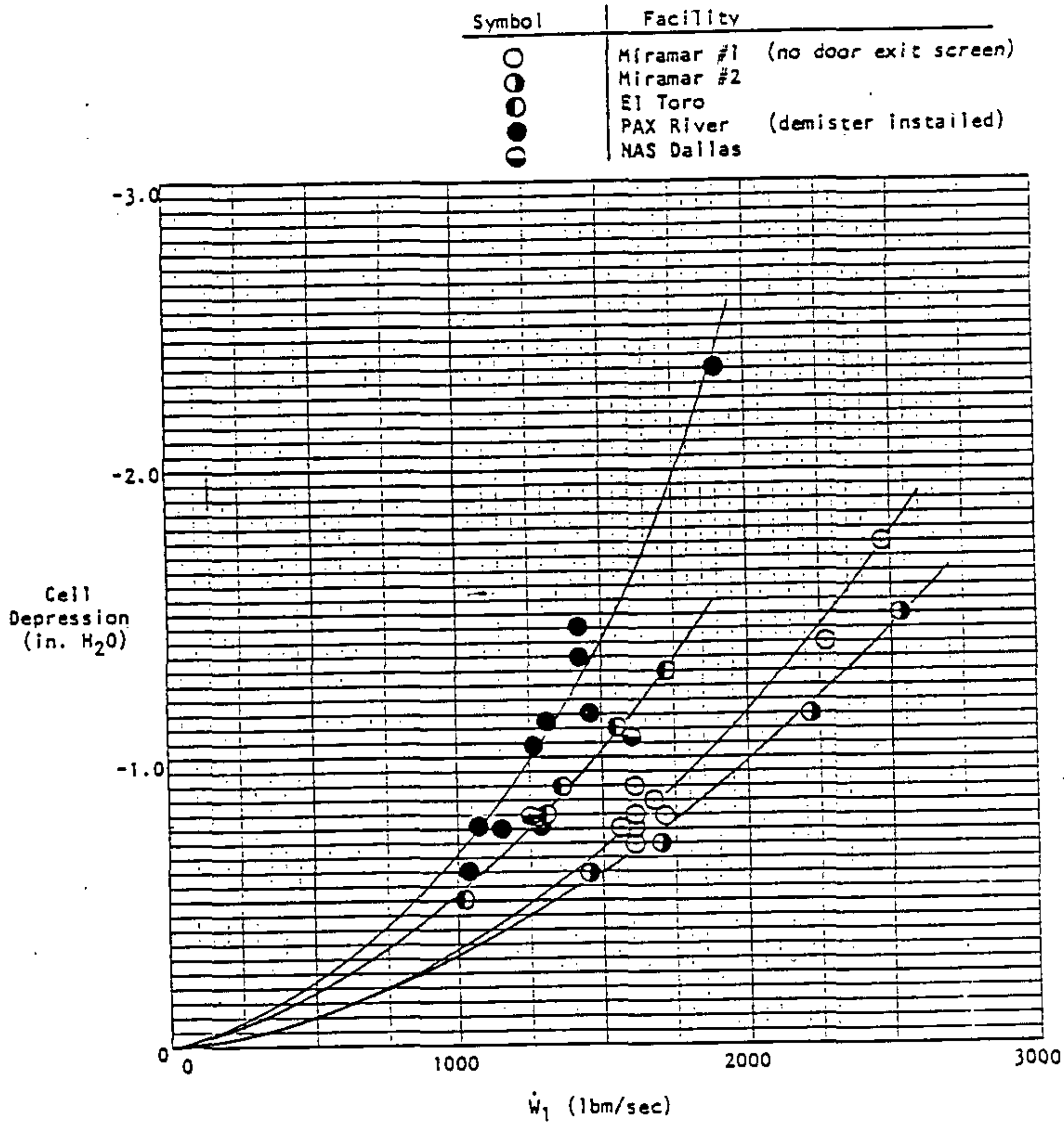

Figure 9
Cell Depression Versus Primary Inlet
Flow Rate for Various Facilities

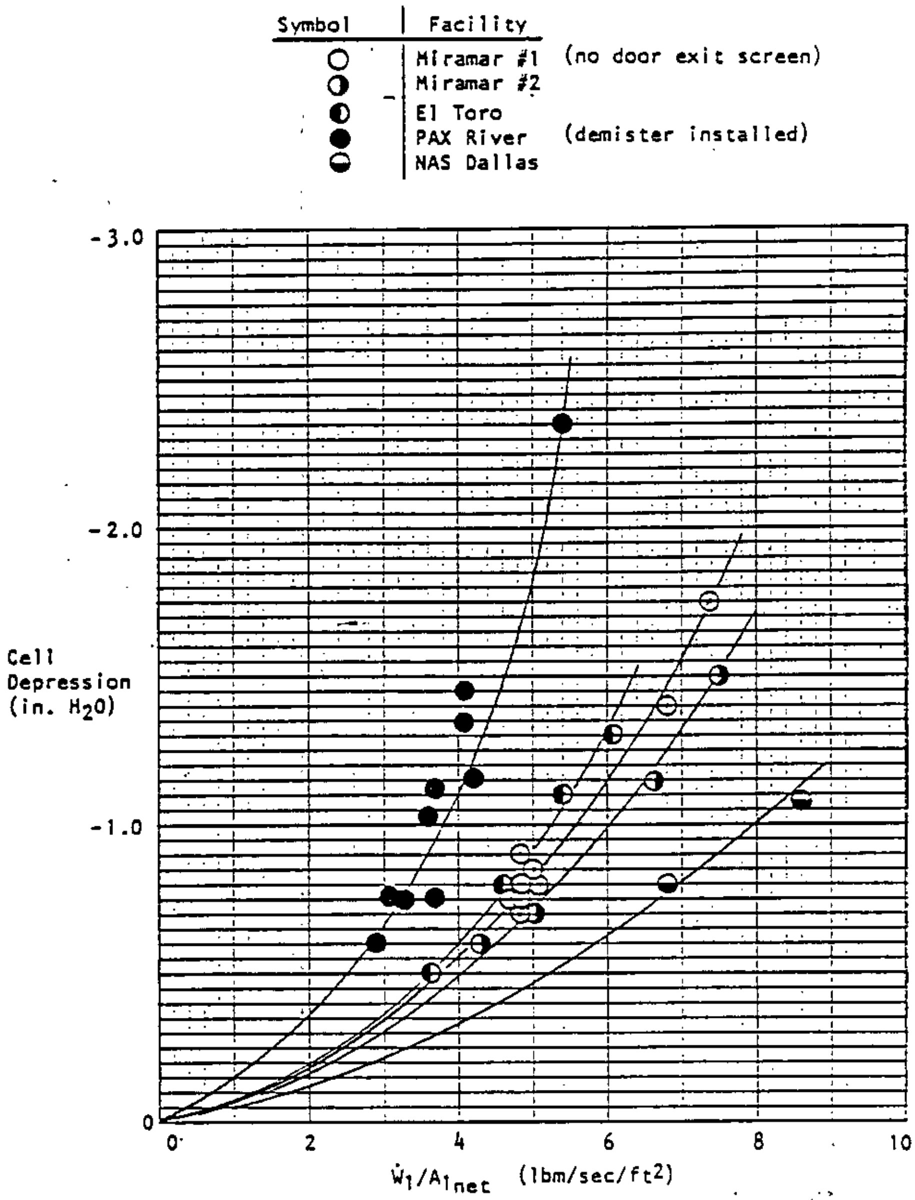

Figure 10
Cell Depression Versus Primary Inlet Specific Mass Flow Rate for Various Facilities

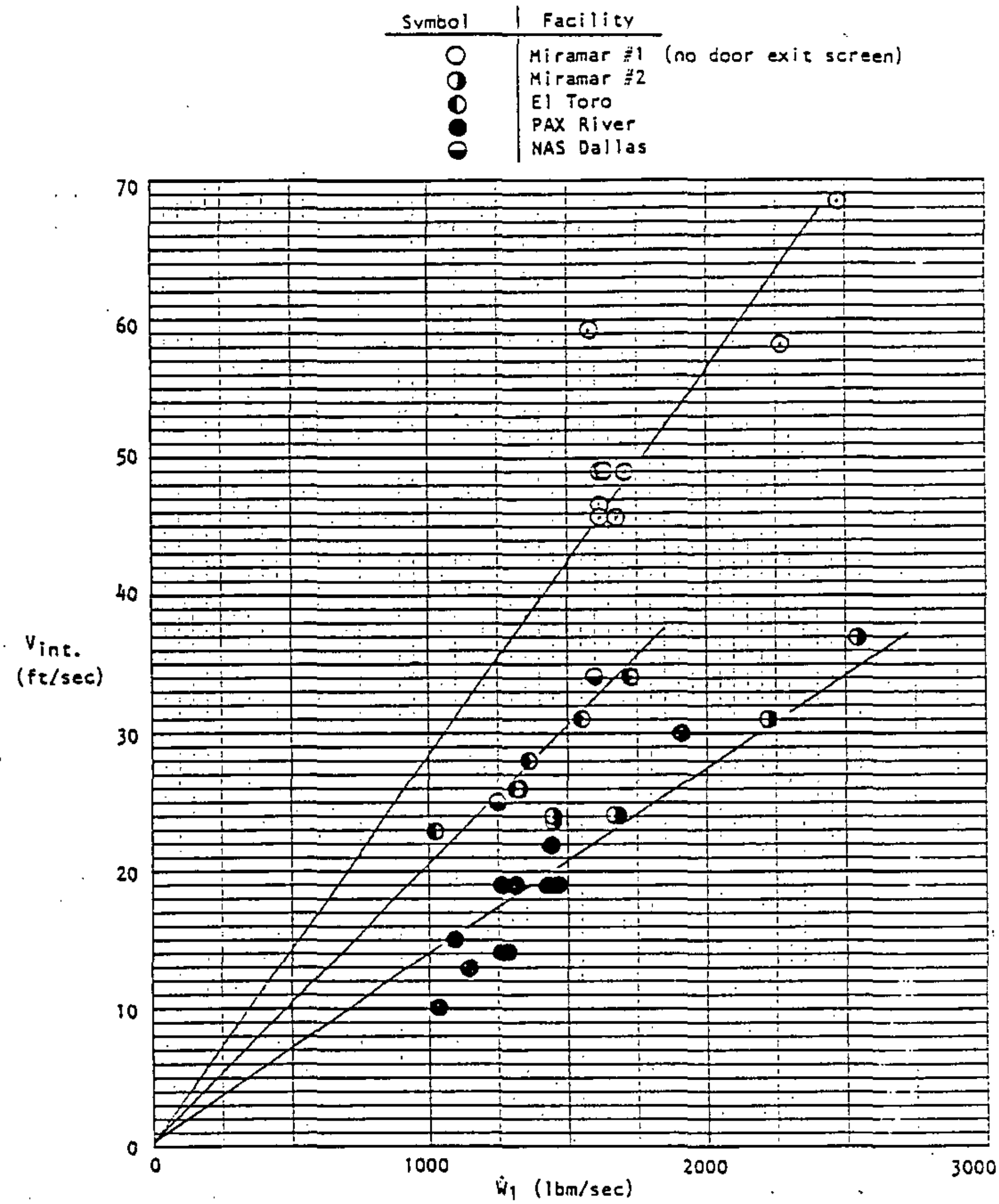

Figure 11
Enclosure Interior Velocity Versus Primary Mass Flow Rate for Various Facilities

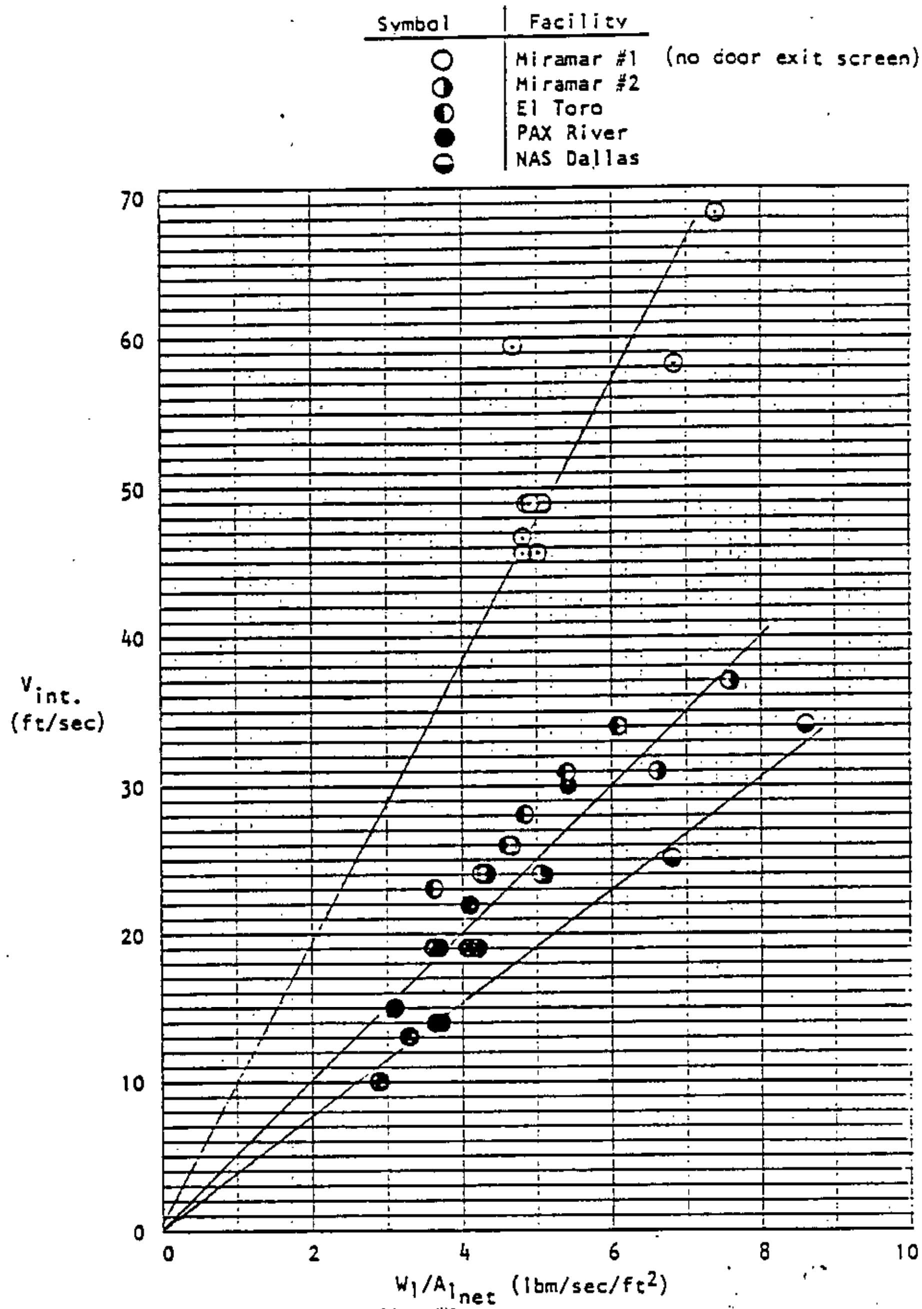

Figure 12
Enclosure Interior Velocity Versus Primary Inlet Specific Mass Flow Rate for Various Facilities

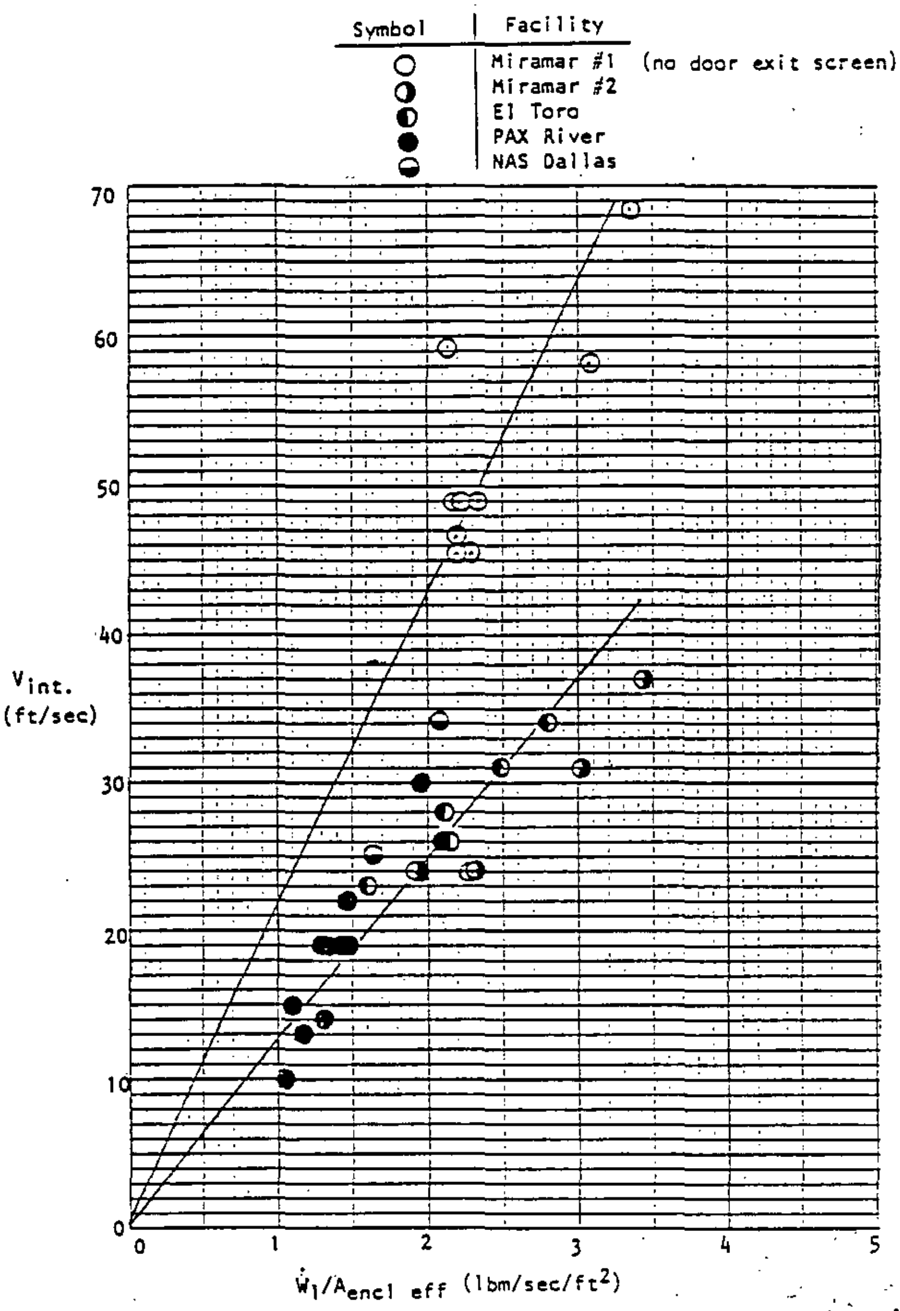

Figure 13
Enclosure Interior Velocity Versus Door Outlet Specific Mass Flow Rate

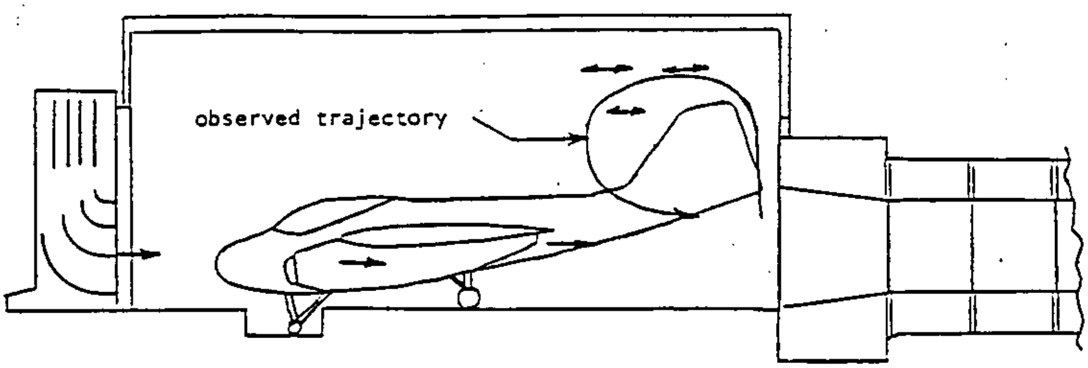

A. Side Elevation

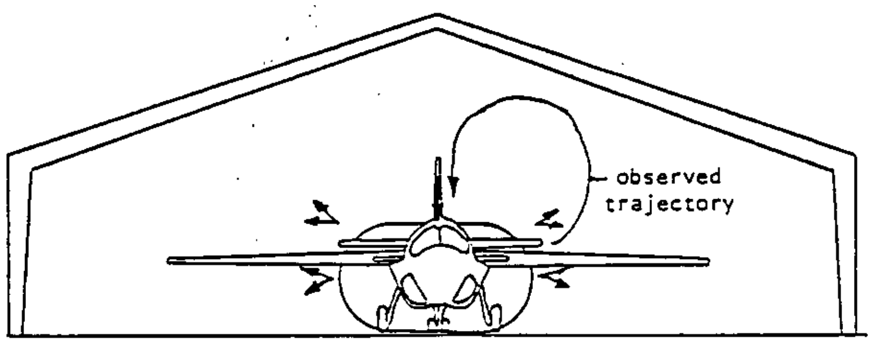

B. Front Elevation
(backwall streamer pattern)

Figure 14
El Toro Internal Flow Patterns with the A-6 Aircraft

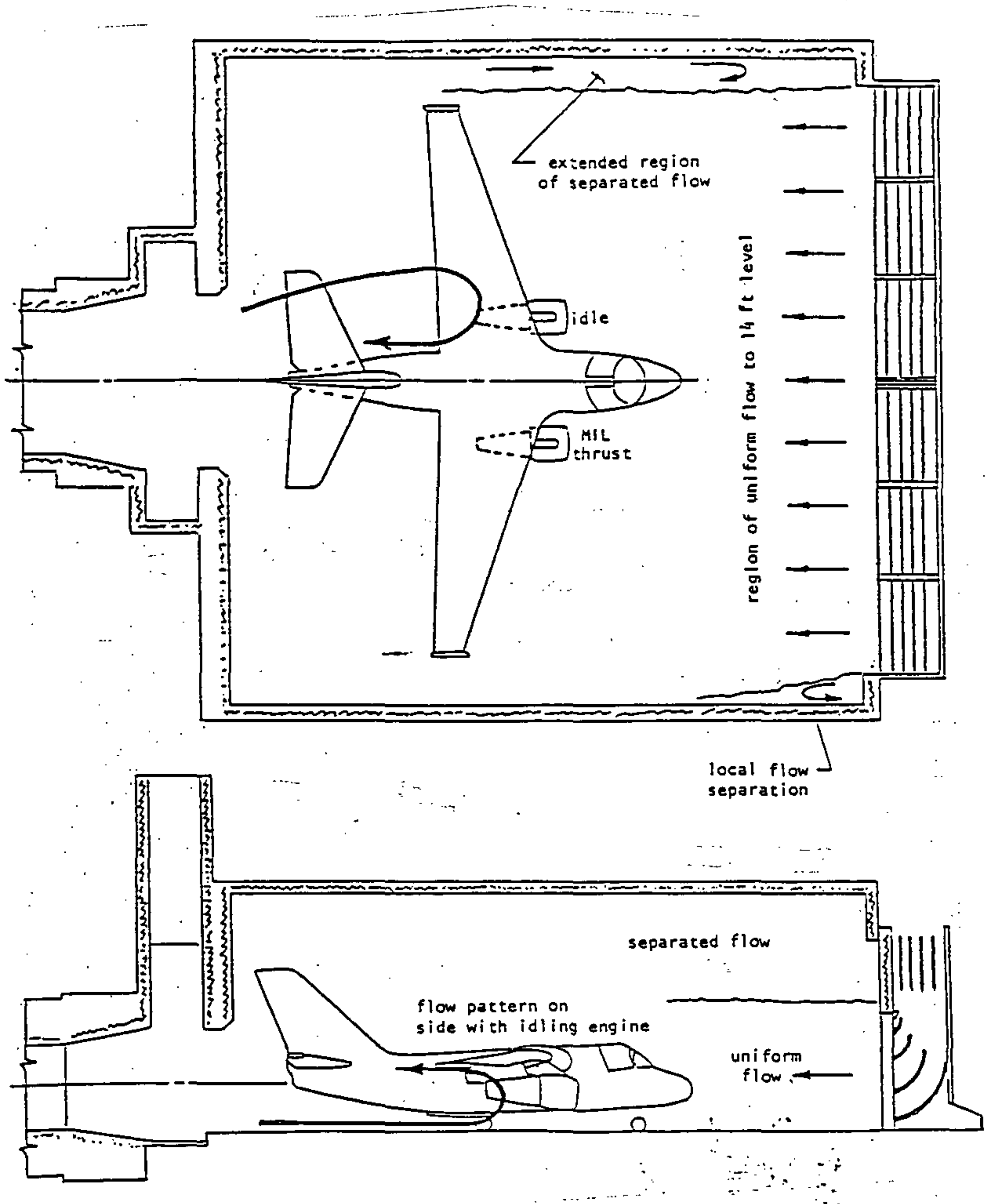

Figure 15
Patuxent River Internal Flow Patterns
with the S-3A Aircraft

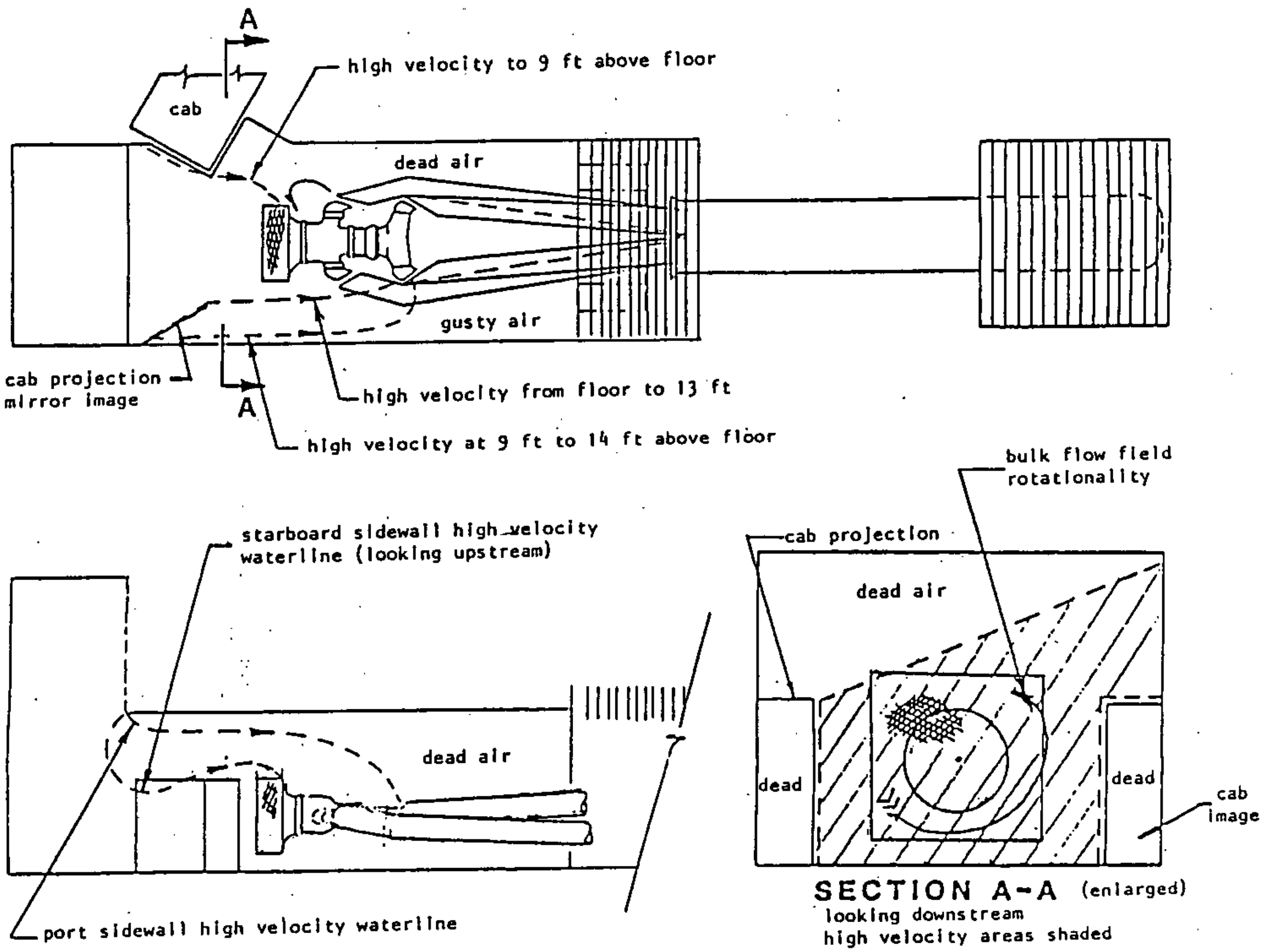

Figure 16
Cherry Point Engine Test Cell Internal Flow Patterns
with the Pegasus Engine

Section 8: AUGMENTER WALL TEMPERATURE

8.1 Wall Temperature Measurement. (For definitions of the terms for equations below, refer to Table 1.) Measurements of augmenter wall temperature were made in all of the postconstruction facility checkouts reported herein [1, 3, 8, 9]. In addition, measurements of augmenter wall temperature were made during the model test programs reported in References [3, 14 and 15]. In some cases the augmenter wall temperature data have been reduced to a wall temperature parameter where:

EQUATION: $$T_p = \frac{T_{wall} - T_{ambient}}{T_{T_{N(8)}} - T_{ambient}} \qquad (1)$$

Measured wall temperatures are plotted versus axial position in the augmenter in Figures 17, 18 and 19 for aligned engines or aircraft. Figures 17 and 18 present such data for aligned aircraft and engine cases where the exhaust centerlines were aligned with and nearly contiguous with the augmenter centerline. As a good first approximation, the maximum augmenter wall temperature in such cases equals the mixed exhaust temperature where:

EQUATION: (2)

$$T_{mix} = \frac{\dot{W}_E \times C_{P_E} \times T_{T_{N(8)}} + (\dot{W}_{IT} - \dot{W}_E) \times C_{P_{air}} \times T_{amb}}{C_{P_{augm\ exh}} \times \dot{W}_{IT}}$$

Typical conditions are:

$C_{p\ air}$ = 0.24 Btu/lb° F (R)

T_{amb} = 100° F maximum

Thrust Setting	$T_{T_{N(8)}}$ ° F	C_{P_E}	$C_{P_{aug\ exh}}$
Mil	1200	0.27	0.25
A/B	3200	0.34	0.26

8.1.1 Wall Temperature with Outward-Splayed Exhaust. Figure 19 contains data for aligned aircraft where the exhaust centerlines were splayed outward and located a significant lateral distance from the augmenter centerline (A-6, F-14A and S-3A). In addition, Figure 19 contains a projected wall temperature distribution for the F-14A in a Miramar type hush-house based on the model tests [3]. The projection based upon the model tests is quite accurate.

EQUATION: ($T_{wall\ max\ projected}$ = 1020° F, $T_{wall\ max\ meas}$ = 980° F) (3)

8.1.2 Wall Temperature with Aircraft Misalignment. Figure 19 also shows the 150° F (65.6° C) lower wall temperature measured at Patuxent River during

				Facility	
Aircraft/Engine	Y_0	α_s	T_{tN} (°F)	Dallas	El Toro
Bare/J-79	0	0°	1140 (MIL)	◒	
Bare/J-79	0	0°	3040 (A/B)	◒~	
A-4/J-52	0	0°	1420 (MIL)		X

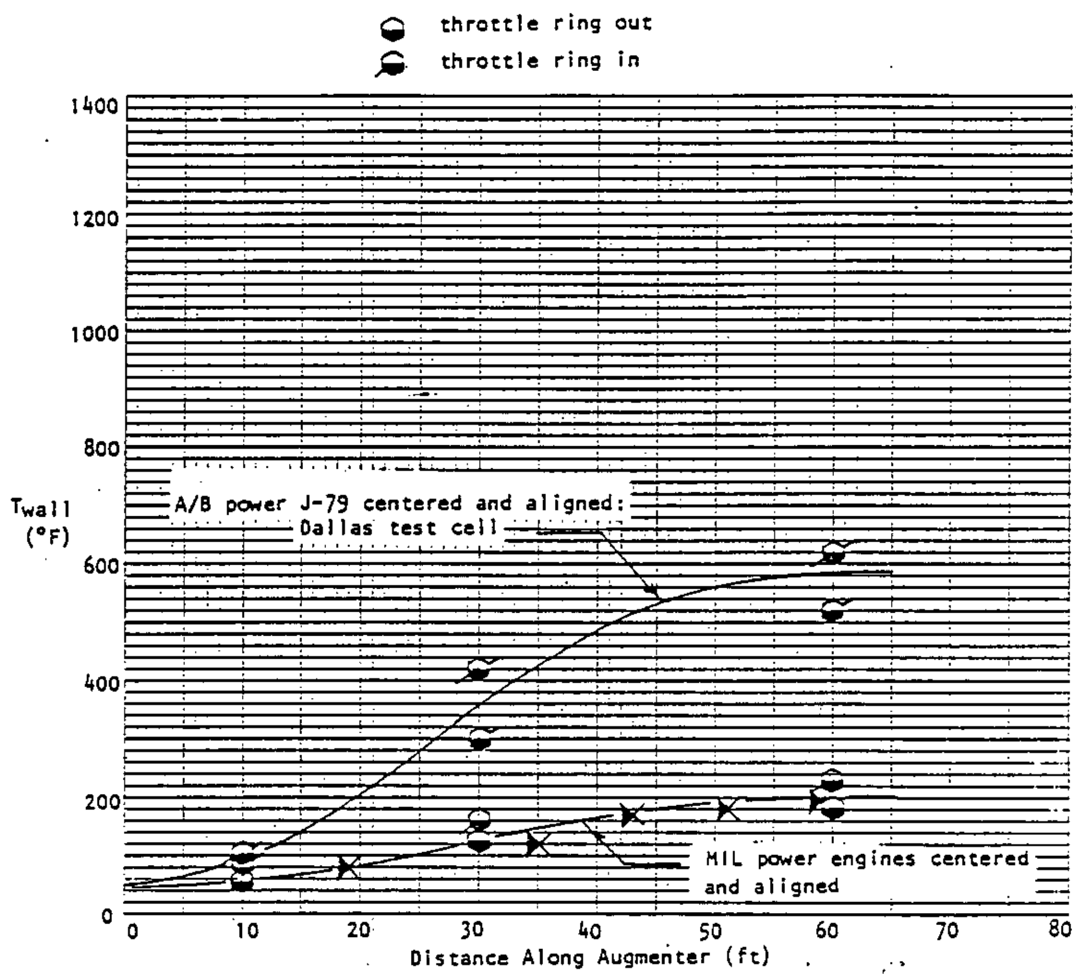

Figure 17
Augmenter Wall Temperature Distributors for Various Facilities with Centered and Aligned Engine

Aircraft/engine	Y_o	α_s	T_{t_N} (°F)	Facility: MM #2	Facility: El Toro	Facility: PAX
F-4/J-79	.21	0°	1140 (MIL) 3040 (A/B)	◑		●
F-4/J-79	.28	0°	1140 (MIL)		◐	

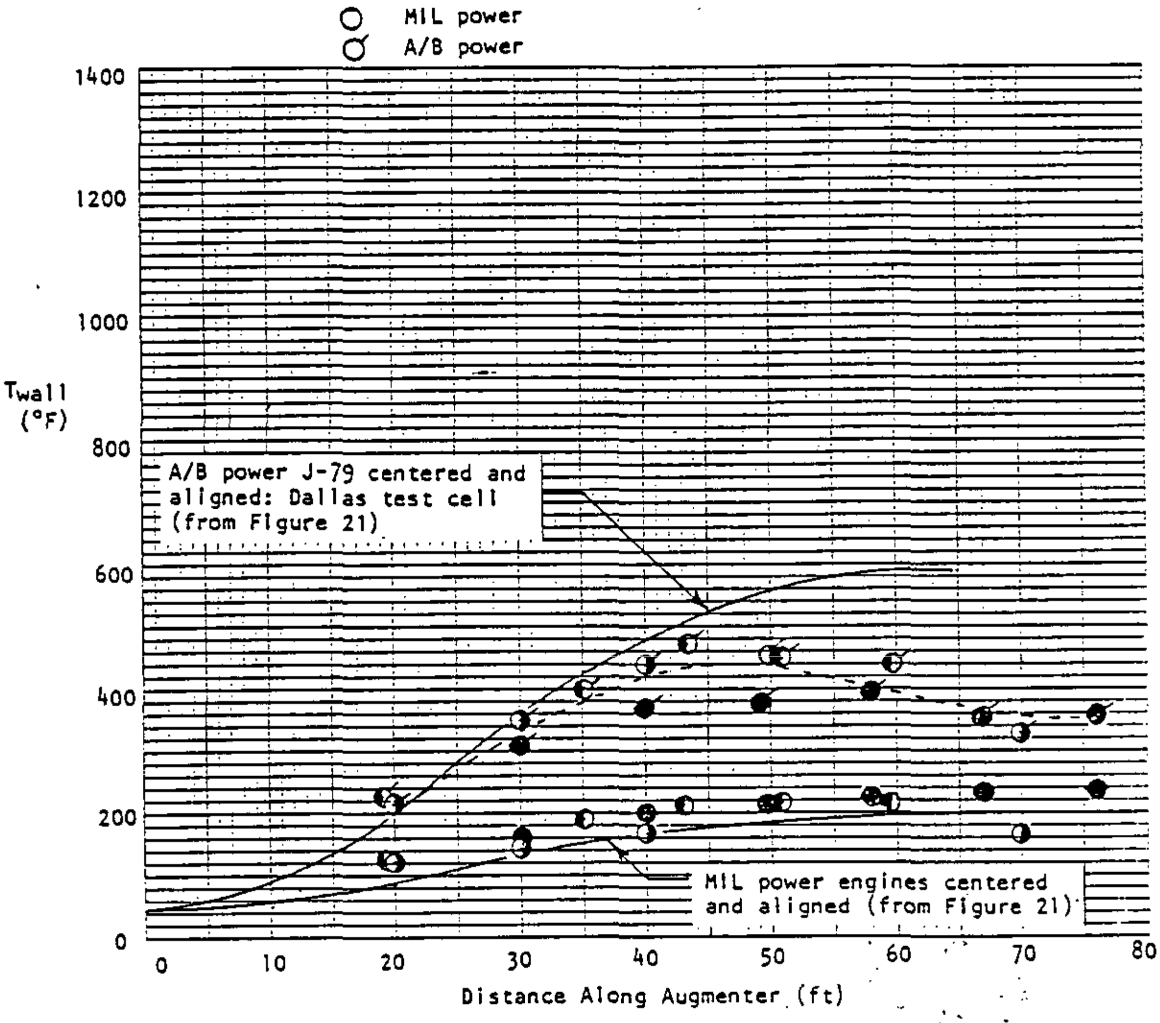

Figure 18
Augmenter Wall Temperature Distributions for Various Facilities with J-79 Powered F-4 (Single Engine Operation)

Aircraft/Engine	Y_p	α_s	T_{t_N}(°F)	Facility: MM #1	MM #2	El Toro	PAX
A-6/J-52	.51	6°	1180(MIL)			◐	
A-6/J-52	.37	6°	1180(MIL)				●
F-14A/TF-30	.47	1°	940(MIL)		△		▲
F-14A/TF-30	.47	1°	3140(A/B)	△	△		▲*
S-3A/TF-34	.82	0°	540(MIL)				◆

*note: data obtained with temperature sensitive paint

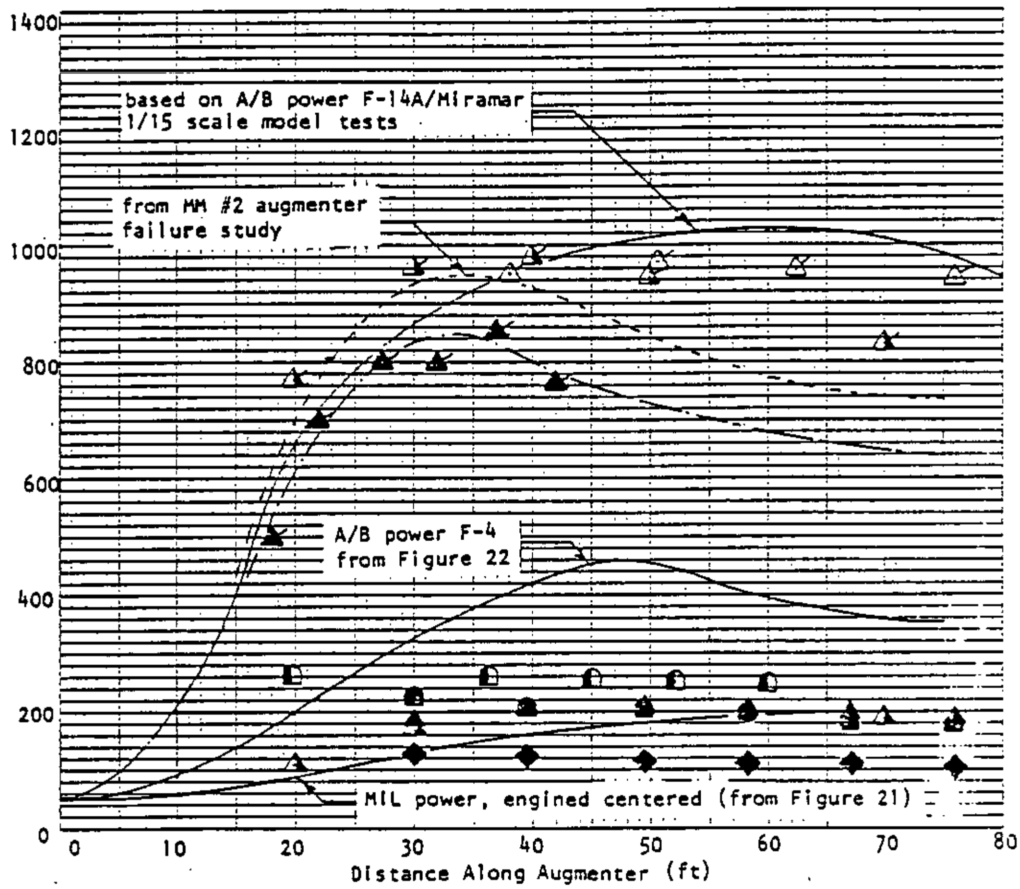

Figure 19
Augmenter Wall Temperature Distribution for Various Facilities Showing the Effect of Significant Engine Centerline Lateral Offset and Misalignment (Single Engine Operation)

F-14A misalignment tests run in Miramar Hush-House No. 2 and reported in Reference [6] and those run at Patuxent River are summarized in Figure 20. This shows the rapid increase in maximum augmenter wall temperature with aircraft misalignment. Figure 20 further shows the beneficial effect of the flared augmenter inlet on wall temperatures in the Patuxent River hush-house.

8.1.3 Wall Temperature/Engine Nozzle Distance Correlation. Figures 21 and 22 represent an attempt to relate maximum augmenter wall temperature with the distance from the engine nozzle exit to the impingement point. In Figure 21, maximum wall temperature parameter, $^{T}P_{max}$, is plotted versus the distance from the nozzle exit to the nondimensionalized location of maximum wall temperature within the augmenter (this basically portrays the effect of jet mixing). Figure 22 presents the relationship between hot spot location and the point at which the projected nozzle centerline intersects the augmenter wall. Figures 21 and 22 are particularly useful in cases where the nozzle centerline is canted toward the augmenter wall or where the nozzle centerline is offset significantly from the augmenter centerline. Even so, Figures 21 and 22 do not account for effects on pumping, such as those derived from the application of a flared augmenter inlet to the Patuxent River hush-house.

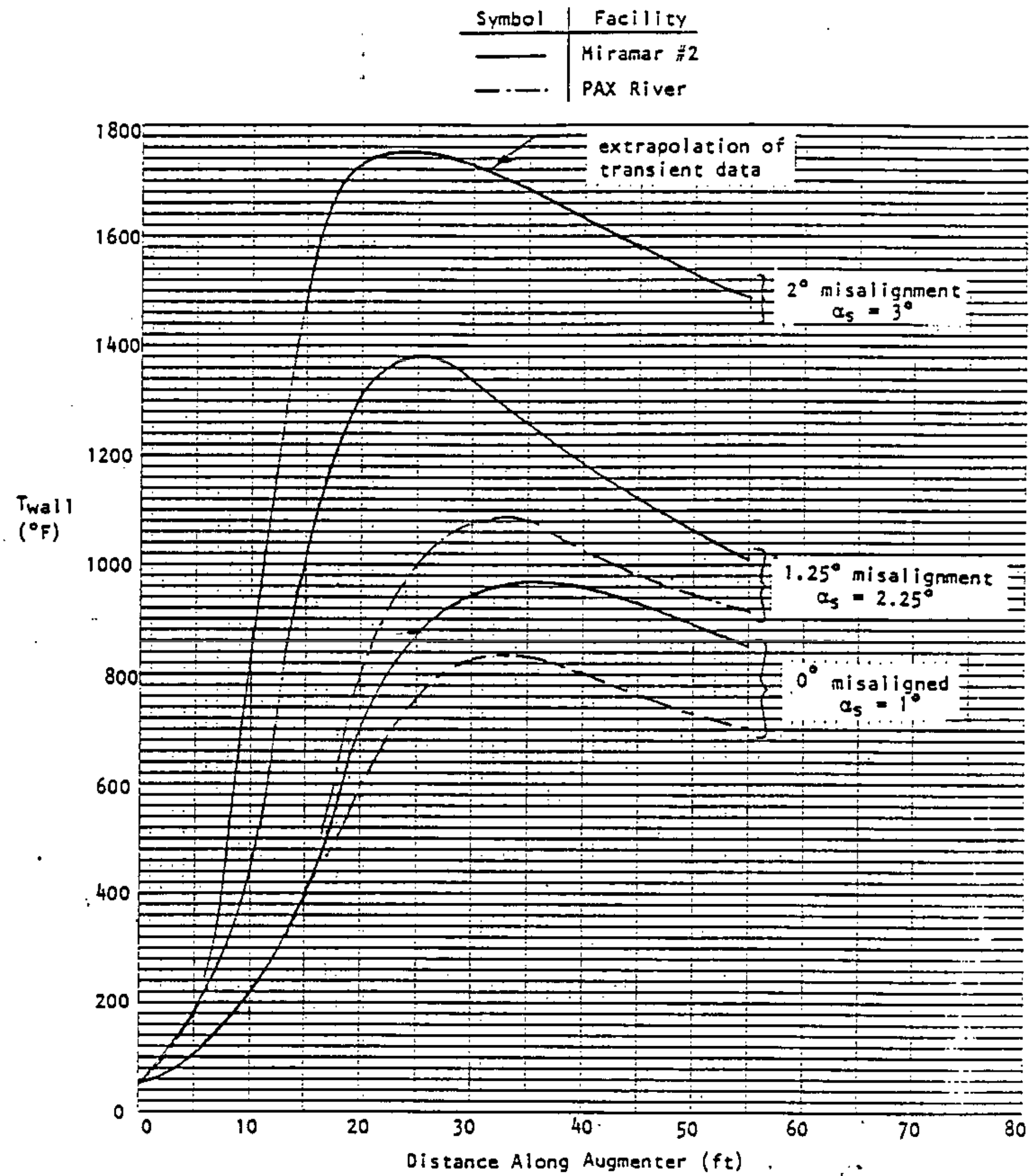

Figure 20
Augmenter Sidewall Temperature Distribution for F-14A Operation with One Engine in A/B at Various Degrees of Aircraft Misalignment (Sidewall Nearest Operating Engine)

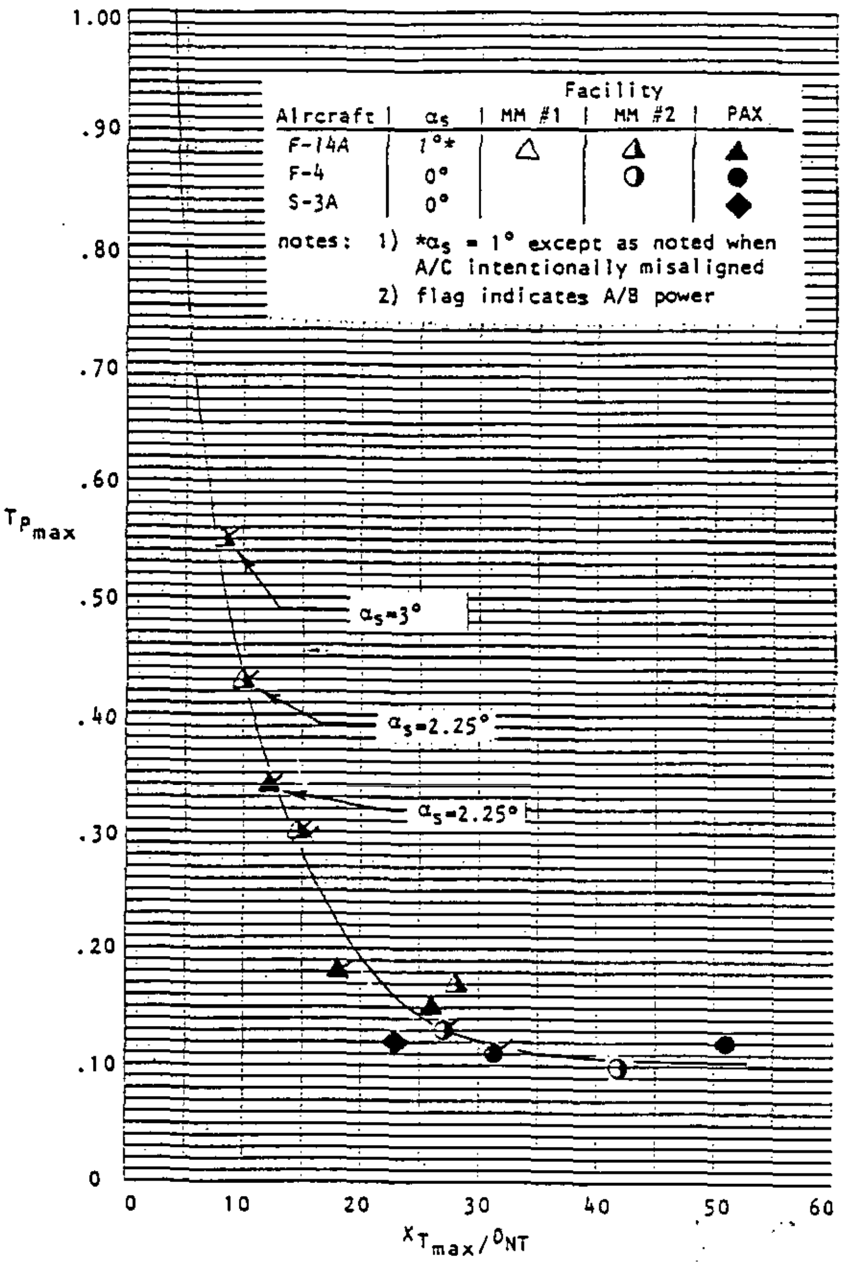

Figure 21
Maximum Augmenter Wall Temperature Parameter for Various Facilities Showing the Effect of Engine Centerline Lateral Offset and Misalignment (Single Engine)

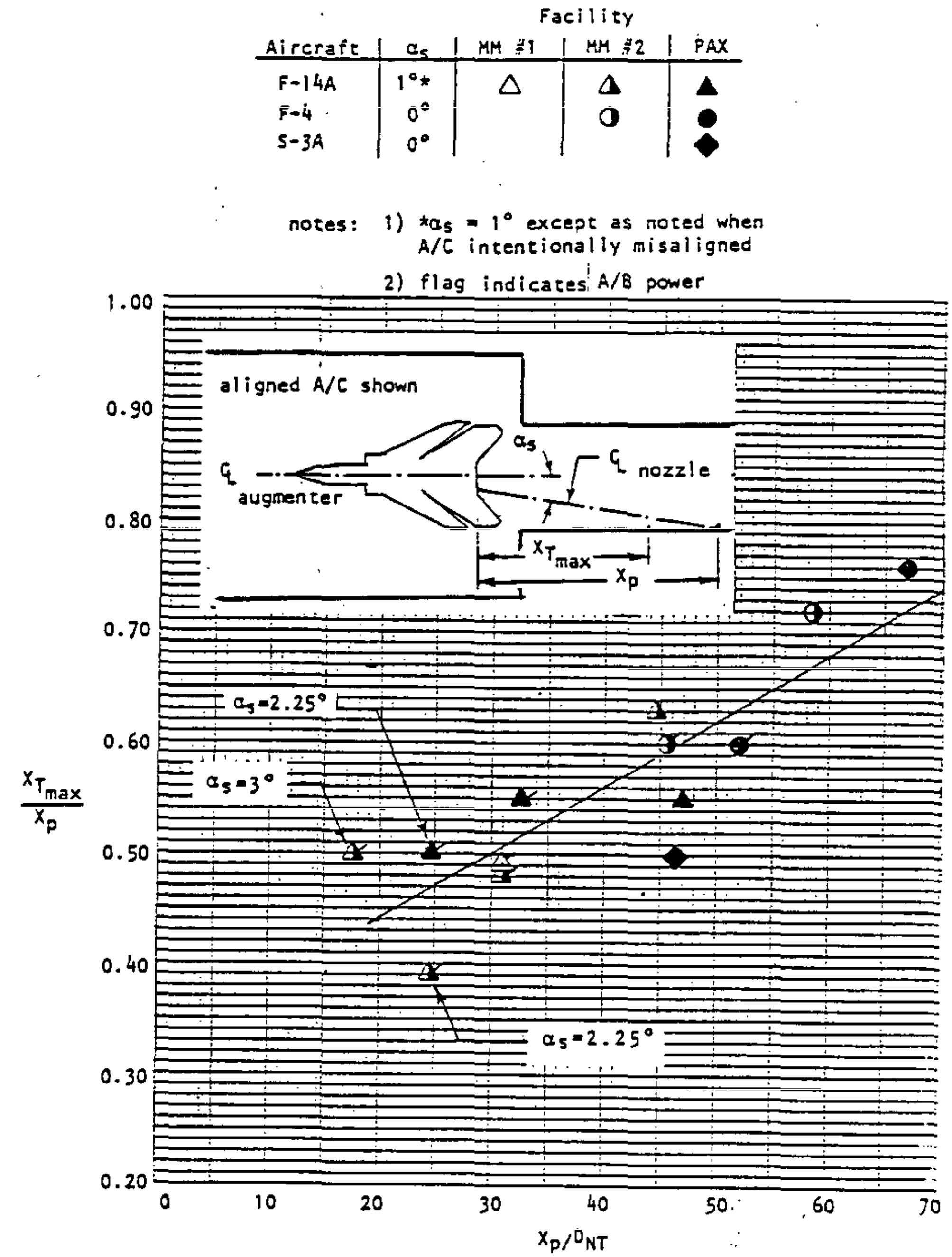

Figure 22
Axial Location of Maximum Augmenter Wall Temperature in Various Facilities for Aligned and Intentionally Misaligned Aircraft

Section 9: AUGMENTER EXIT VELOCITY

9.1 Exit Velocity Limits. Augmenter exit velocity measurements were taken in the postconstruction checkout tests reported in References [1, 3, and 8] and in model tests reported in References [3, 13 and 14]. Velocities were derived from measurements of augmenter exit total pressure and total temperature assuming that the static pressure across the augmenter exit plane was uniform and equal to ambient (barometric) pressure. Augmenter exit velocity is important because the flow leaving the augmenter is an important noise source. For all of the facilities (which were designed to meet an 85 dBA noise limit at 250 ft (76.2 m) from the engine exhaust plane), the intent was that the "self-noise" caused by flow leaving the augmenter exit shall not contribute more than 2 dBA to the maximum noise level at the 250-ft distance. This implied limiting the peak velocity in the flow which leaves the augmenter to less than 500 f/s (152.4 m/s). A much lower exit velocity, 350 f/s (106.7 m/s), will be required to meet a noise limit of 75 dBA at 250 ft with a lined augmenter plus a ramp-type sound suppressor.

9.2 Exit Velocity Test Results. All of the full-scale augmenter exit velocity distributions measured are presented in Figures 23 and 24. Figure 23 contains data from the checkouts of the Miramar No. 2 and El Toro hush-houses. Figure 24 contains data taken with a J-79 in the NAS Dallas test cell. Figure 24 shows the effect of throttling (reducing augmentation) on the augmenter exit velocity. This would normally have resulted in a lower maximum noise level at 250 ft, but the throttle ring generated noise so the total noise level increased.

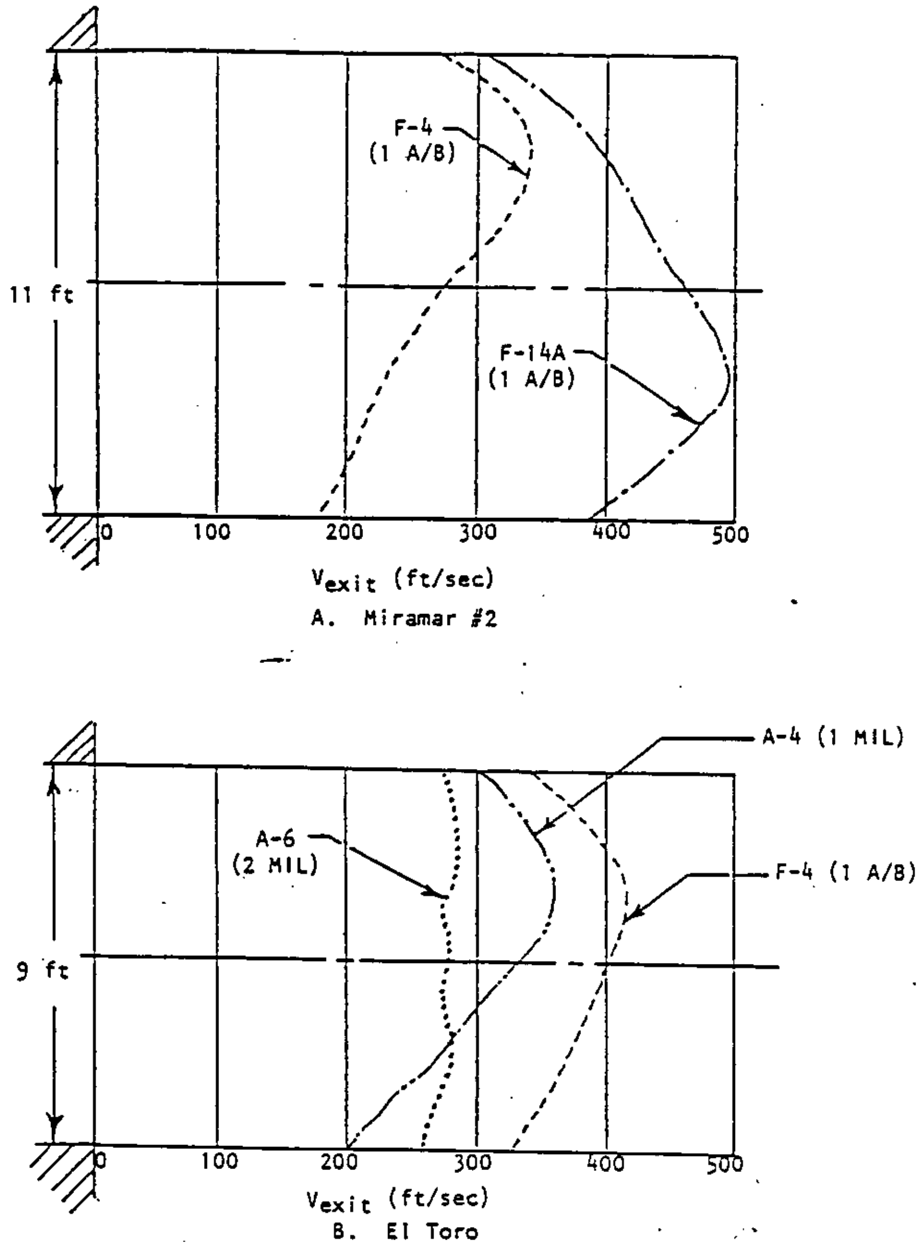

Figure 23
Miramar and El Toro Augmenter Exit Velocity Distributions

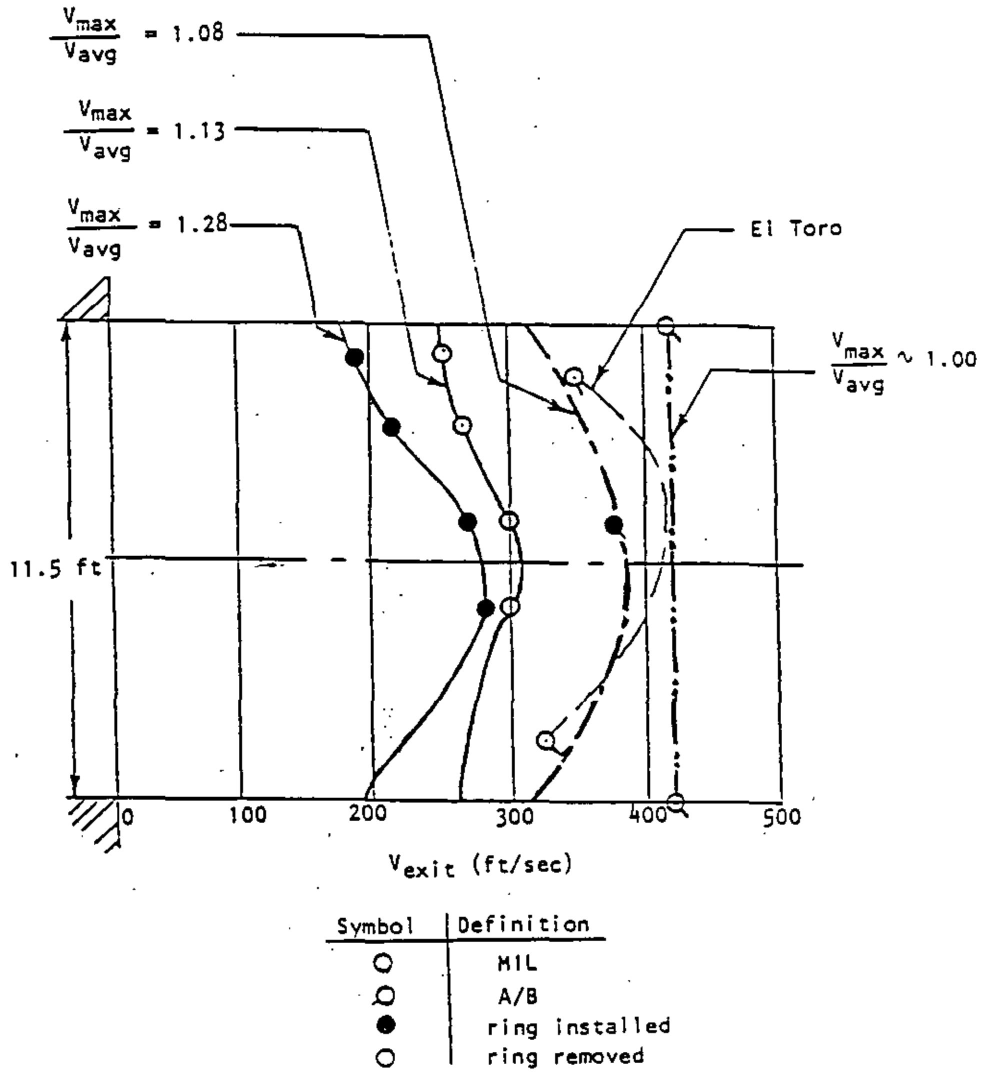

Figure 24
NAS Dallas Engine Test Cell Augmenter Exit
Velocity Distributions

Section 10: VISIBLE EMISSIONS

10.1 Studies on Minimizing Visible Emissions. In 1980, the Navy sponsored a program to study ways of minimizing visible emissions from test cell and hush-house installations to meet a Ringelmann 1.0 (20 percent) opacity criteria during all runups. The study involved full-scale exhaust plume observations [5] and model-scale tests using a smokey jet [12]. For the full-scale observations and predictions, the opacity of the open air jet was chosen as the reference value. This opacity (defined in terms of Ringelmann number) does not diminish due to typical jet mixing because, while the particulate concentration decreases, the effective plume diameter increases. The reference open air jet opacities of several engines are presented in Table 6:

Table 6
Open-Air Jet Opacities

AIRCRAFT	ENGINE	POWER SETTING	JET RINGELEMANN NO.
A-4	J-52 P408	Mil	0.75
A-6	J-52 P8	Mil	0.50
A-7	TF-30 P6	Mil	2.25
	TF-41 A2	Mil	1.25
F-4	J-79 GE8, 10A	Mil	2.50
		A/B	0.75
	J-79 GE10B, C	Mil	0.50
		A/B	0.50
F-8	J-57 P420	Mil	0.50
		A/B	0.25
F-14A	TF-30 P412	Mil	0.50
		A/B	0.50

10.2 Model-Scale Test Conclusions. The following conclusions were derived from the observations and model-scale tests:

a) Maximum exhaust plume opacity typically occurs during engine runup in maximum nonafterburning thrust.

b) At maximum nonafterburning thrust, the open-air jet opacity of most engine exhausts is below Ringelmann 1.0 (the important exceptions being older J-79's and the TF-41).

c) It does not appear practical to design an exhaust system that exhibits a plume opacity less than that of an open-air jet.

d) The jet mixing and deceleration process, typical of a low-loss, straight-through augmenter plus ramp, yields an exhaust plume opacity only slightly greater than that of an open-air jet.

e) The limited dilution and subsequent deceleration typical of most test cell exhaust systems, can result in an exhaust plume opacity many times that of an open-air jet.

Section 11: ENCLOSURE INTERIOR NOISE

11.1 Introduction. This section deals with the interior noise of hush-houses and jet engine test cells. The data reported were obtained either by the performance evaluation of completed full-scale facilities or by model-scale experimental studies. Many key acoustical results of checkout measurements and model studies are included. The structure of aircraft during ground runup in hush-houses or that of engines during out-of-airframe tests in a jet engine test cell may experience sound and sound-induced vibration that differs from that obtained when the test is run outdoors.

Note: certain parts of aircraft are frequently exposed to substantially higher noise levels than those encountered during ground runup outdoors. This occurs when aircraft are taking off pairwise on the same runway and when they are parked on the deck of an aircraft carrier during the takeoff of other aircraft.

11.1.1 Enclosure Interior Noise Sources. The sources of enclosure interior noise are the engine intake and the engine exhaust. While all the engine intake noise enters the enclosure, only a part of the engine exhaust noise "spills" into the enclosure. The larger the distance between the engine exhaust plane from the augmenter entrance, X_N, and the smaller the equivalent diameter of the augmenter, D_A, the larger portion of the engine exhaust noise reaches the enclosure. The sound field inside of the enclosure is made up from the direct sound radiated from the engine and from the reflections of the direct sound from the enclosure interior surfaces.

The enclosure interior noise is of concern because of:

a) Sound induced vibrations of the aircraft, engine components and the structure of the enclosure

b) Its potential impact on the hearing of operating personnel

c) Sound radiation through the enclosure walls and intake muffler to the outside and through the viewing window to the control room.

The interior noise data obtained in full-scale test facilities are compiled in Table 7. The objectives and key results of model studies are presented in Tables 8A through 8C.

11.2 Enclosure Interior Noise in Full-Scale Test Facilities. The A-weighted interior noise level obtained at standard interior microphone positions is presented in the right column in Table 7. The location of the standard interior microphone positions for the different facilities is shown in Table 9.

11.3 Typical Interior Noise Level Spectra. Figure 25 shows the 1/3-octave band spectrum of the interior noise measured in the Miramar No. 2 hush-house at Standard Interior Microphone Position No. 3 obtained while the port engine of the F-4 and F-14A aircraft was operating at maximum afterburner. Although the F-4 aircraft has an engine of lower sound power output than that of the F-14A aircraft, it produces substantially higher

Table 7
Summary of Far-Field and Interior Noise Levels
of Full-Scale Test Facilities

Facility	Aircraft/ Engine	Power Setting	Exterior Sound Level, dBA* (250 ft Circle) Position[1]							250 ft Maximum Level/ Position of Max. Level	Interior Sound Level, dBA* Position[2]			
			0°	30°	60°	90°	120°	150°	180°		1	2	3	4
Miramar No. 1 Hush-House[3] [3]	F-4J	1 Mil	76	77[4]	77[4]	75	74	76	71	76[4]/150°	129	130	132	132
		1 A/B	81	86[4]	86[4]	79	80	81	78	81[4]/150°	135	137	138	137
	F-14A	1 Mil	66	66	67	67	69	73	74	74/180°	112	120	121	124
		1 A/B	75	78	78	77	81	84	85	85/180°	134	133	136	138
Miramar No. 2 Hush-House [1, 22]	F-4N	1 A/B	74	74	79	75	81	80	74	81/120°	134	–	139	141
	F-14A	1 A/B	71	73	74	77	84	86	82	86/150°	132	–	136	138
	F-18	1 Mil	76	67	–	–	73	–	78	–	129	131	–	–
		1 A/B	81	72	–	–	81	–	83[8]	–	135	135	–	–
El Toro Hush-House [1]	F-4	1 A/B	73	76	77	76	78	83	82	83/150°	135	–	141	142
	A-4	Mil	68	71	71	71	75	83	84	84/180°	135	–	140	142
	A-6	Both Mil	76	78	79	78	78	84	94	94/180°	137	–	143	145

*Rounded to nearest dB.

Table 7 (Continued)
Summary of Far-Field and Interior Noise Levels
of Full-Scale Test Facilities

Facility	Aircraft/ Engine	Power Setting	Exterior Sound Level, dBA* (250 ft Circle) Position[1]							250 ft Maximum Level/ Position of Max. Level	Interior Sound Level, dBA* Position[2]			
			0°	30°	60°	90°	120°	150°	180°		1	2	3	4
Patuxent Riv.	F-4J	1 Mil	68	65	68	69	76	76	72	76/150°	127	–	–	137
Hush-House		Both Mil	70	67	70	73	78	78	76	78/150°	130	–	–	140
[9, 23]		1 A/B	72	70	76	75	80	81	76	81/150°	133	–	–	144
	F-14A	1 Mil	63	60	63	65	72	74	74	74/180°	124	–	–	125
		Both Mil	63	62	64	68	76	80	80	80/180°	124	–	–	128
		1 A/B	72	70	73	74	79	84	83	84/150°	132	–	–	138
		Both A/B	76	74	76	77	86	88	90	90/180°	133	–	–	140
	S-3A	1 Mil	62	59	60	58	58	59	60	62/0°	124	–	–	128
		Both Mil	67	63	64	61	63	65	66	67/0°	127	–	–	128
	A-6	1 Mil	68	66	67	68	70	72	82	82/180°	130	–	–	130
		Both Mil	72	70	69	70	73	76	86	86/180°	140	–	–	142
Dallas Test	J79-GE-8D	Mil[5]	73	71	72	77	80	83	85	85/180°	133	–	138	–
Cell [24, 25]		Mil[6]	71	69	71	76	79	82	84	84/180°	133	–	138	–
		A/B[5]	78	80	80	83	90	89	94	94/180°	139	–	143	–
		A/B[6]	78	78	79	83	89	89	93	93/180°	139	–	143	–
N. Island Test	J79-GE-8D	Mil	62	69[7]	64[7]	63[7]	66[7]	70	68	70/150°	–	–	141	–
Cell 20 [19]		A/B	70	75[7]	71[7]	70[7]	73[7]	77	76	77/150°	–	–	143	–

*Rounded to nearest dB.

Table 7 (Continued)
Summary of Far-Field and Interior Noise Levels
of Full-Scale Test Facilities

Facility	Aircraft/ Engine	Power Setting	Exterior Sound Level, dBA* (250 ft Circle) Position[1]							250 ft Maximum Level/ Position of Max. Level	Interior Sound Level, dBA* Position[2]			
			0°	30°	60°	90°	120°	150°	180°		1	2	3	4
Alameda Test Cell No. 15 [26]	TF41-A2B	Mil	64[7]	71	67	66	67	73	67	73/150°	–	–	138	–
	J57-P10	Mil	62[2]	69	64	64	67	72	65	72/150°	–	–	137	–
Lemoore Coanda Cell Port											Midway Between Engine Test Center Line & Wall			
[20]	TF30-P408	Mil	88	84	83	83	88	86	92	92/180°			141	
	TF41-A2B	Mil	88	85	83	84	87	86	87	88/0°			–	
	F-404	Mil	92	87	87	87	91	90	92	92/0° & 180°			143	
		A/B	92	88	87	88	92	91	93	93°/180°			142	

*Rounded to nearest dB.

Table 7 (Continued)
Summary of Far-Field and Interiir Noise Levels
of Full-Scale Test Facilities

Notes:

1 Position is 250 ft (76.2 m) from engine exhausts: 0° is forward, 180° is aft. Microphones are on the same side of aircraft centerline as is the operating engine.

2 Positions are approximately on a line parallel to the engine axis. Position 4 is approximately in the plane of the engine exhaust for F-4; position 3 is approximately mid-engine; position is forward in the cell; position is between positions 1 and 3.

3 Measurements at Miramar No. 1 were performed every 14° around 250-ft circle. Data are tabulated for closest standard position; except, data for 90° are average of data from measurements at 83° and 97°.

4 Personnel door was open, resulting in abnormally high levels at these positions. These positions were excluded when tabulating maximum level.

5 Throttle ring installed.

6 Throttle ring removed.

7 Data possibly affected by obstruction (buildings) within or on the 250-ft acircle.

8 A-weighted level affected by "screech", a tone in the noise spectrum, related to interaction of shock fronts, which is an abnormal condition.

Table 8A
Objectives and Key Acoustic Results of Model Studies
Miramar Model Study (October 1975) [3]

ACOUSTIC OBJECTIVES	RESULTS
1. Verify acoustical performance of a full-scale hush-house for F-14 aircraft. 2. Provide design information for future hush-house and test cell designs.	1. Exhaust noise of an F-14 in maximum afterburner was predicted to meet the 85 dBA criteria at 250 ft. 2. a) A method was developed to predict a jet sound power spectrum based on jet total temperature nozzle pressure ratio, and nozzle diameter. b) The division of acoustic energy between the interior and exterior of the hush-house depends strongly on the axial distance between the jet and the augmenter entrance. Increasing this distance resulted in more energy in the interior, and less energy entering the augmenter. c) Augmenter attenuation as a function of axial position of the acoustic lining in the augmenter was found to be approximately independent of position, except that little attenuation occurred at low frequencies in the upstream end of the augmenter (at least partly because low frequencies are generated farther downstream in the jet) and little attenuation occured at high frequencies in the downstream end of the augmenter.

Table 8A (Continued)
Objectives and Key Acoustic Results of Model Studies
Miramar Model Study (October 1975) [3]

ACOUSTIC OBJECTIVES	RESULTS
	d) augmenter attenuation generally increased with increase in jet temperature, due to sound velocity gradients in radial direction which refract energy toward the acoustic lining. e) The model augmenter lining (a thin shell of acoustic material with airspace behind) provided slightly better attenuation than the original Miramar lining (total airspace packed with acoustic material).

Table 8B
Objectives and Key Acoustic Results of Model Studies - Western Electro-Acoustic Laboratory Study 1980 [18]

ACOUSTIC OBJECTIVES	RESULTS
Provide Acoustical Performance date for:	
1. Round vs abround augmenters	1. In a certain frequency range lined augmenters of concentric construction may yield lower sound attenuation than area-equivalent lined augmenters of cross-section.
2. Turning vanes vs rampabround	2. Turning vanes generate substantially more noise than a lined 45° ramp. The noise generated by the turning vanes can be reduced by a lined stack extension to levels similar to those obtained with a lined 45° ramp without a lined stack extension.
3. Ramp modifications	3. The ramp modifications investigated did not result in a noticeable reduction of the net exhaust sound power. No investigations have been carried out to determine whether the modifications influence far field noise at typical far field positions at ground level.
4. Coanda suppressor	4. Coanda surface turning provides measurable noise reduction.

Table 8C
Objectives and Key Acoustic Results of Model Studies
Forcing Cone Model Study (June 1983) [14, 17]

ACOUSTIC OBJECTIVES	RESULTS
1. Compare acoustical performance of a round cross section augmenter for the TF-30 and F402 type engine.	1. Attenuation was 3 to 6 dB greater (avg. 4.6 dB) for the F402 below 400 Hz full-scale. Attenuation was 5 dB greater for the TF-30 at 500 and 630 Hz 1/3 octave bands. Attenuation was the same from 800 to 2000 Hz.
2. Determine effect of a "forcing cone" on performance of a round cross-section augmenter for the TF-30 and F402 type engine.	2. Forcing cone produced no acoustical benefits; no change in attenuation for the TF-30; slight degradation for the F402. Forcing cone not recommended acoustical purposes.
3. Determine the effects of two modifications to a standard round augmenter with concentric shell and inner lining: a) completely fill the lower half of the airspace with acoustical material; and b) insert thin vertical acoustical "curtains" into the airspace on both sides of the inner lining.	3. a) Filling the bottom half of the airspace increased the attenuation by 2 to 5 dB between 80 and 160 Hz (full-scale)and decreased the attenuation 1 to 3 dB between 25 and 63 Hz. b) Vertical curtain increased the attenuation 1 to 4 dB between 0 and 60 Hz and did not degrade low frequency attenuation.

Table 9
Location of Standard Microphone Positions for Measuring Interior Noise

FACILITY	INTERIOR POSITION NO. [1, 2]							
	1		2		3		4	
	X ft	Y ft	X ft	Y ft	X ft	Y ft	X ft	Y ft
Miramar No. 1 Hush-House	21	58	21	44	21	30	21	15
Miramar No. 2 Hush-House	21	54	--	--	22	22	21	16
El Toro Hush-House	21	46	--	--	22	22	21	16
Patuxent River Hush-House	21	79	--	--	--	--	25	18
Dallas Test Cell	6	56	--	--	6	15[3]	--	--
North Island Test Cell No. 20	--	--	--	--	6	15[3]	--	--
Alameda Test Cell No. 15	--	--	--	--	6	15[3]	--	--

1 X is the distance of the microphone from the centerline of the hush-house/test cell in feet.

2 Y is the distance of the microphone from the rear interior wall in feet.

3 Approximate.

interior noise levels at this specific measurement position. This is because the distance between the plane of the engine exhaust and the augmenter entrance, X_N, is much larger for the F-4 than it is for the F-14A. Consequently, the F-4 "spills" more of the exhaust sound power into the enclosure than does the F-14A.

Interior noise levels in certain hush-houses and jet engine test cells have been measured also at positions which differ from the standard, such as: (1) near to the front door, (2) near to the observation window, (3) in the control room; and (4) inside the primary and secondary air inlets. The data obtained in these nonstandard positions are documented in Experimental Evaluation of the NAS Miramar Hush-House, [21], Noise from F-18 and F-14 Aircraft Operating in Hush-House #2 Naval Air Station Miramar, [22], Noise Levels of the NAS Patuxent River, Maryland Hush-House [23].

11.4 Enclosure Interior Noise Studies Utilizing Scale Models. A systematic scale model study [3] has been carried out to identify how the sound power of a model jet splits between the enclosure and the augmenter tube. It was found that the key parameter that controls the split of the jet sound power between the enclosure and the augmenter is the ratio X_N/D_A, where X_N is the distance between the nozzle exhaust plane and the augmenter entrance, and D_A is the equivalent diameter of the augmenter entrance.

Figure 26 shows the split of the jet sound power between the enclosure (burner room) and the augmenter (exhaust room) measured by Reference 3 on 1/15-scale model of a hush-house. The parameters X_N and L_A represent the nozzle pressure ratio and the length of an unlined augmenter tube.

Figure 27 shows how the sound power that is radiated into the enclosure (burner room) increases with increasing X_N the distance between the nozzle exhaust plane and the augmenter entrance. The conditions depicted in Figure 27 span a X_N/D_A ratio range from 0.04 to 1.44.

NOTE: No systematic model studies were carried out to date to investigate the spatial distribution of the interior noise level. To be realistic, such model studies will need to utilize a model-scale engine that represents both the intake and exhaust noise of a full-scale engine.

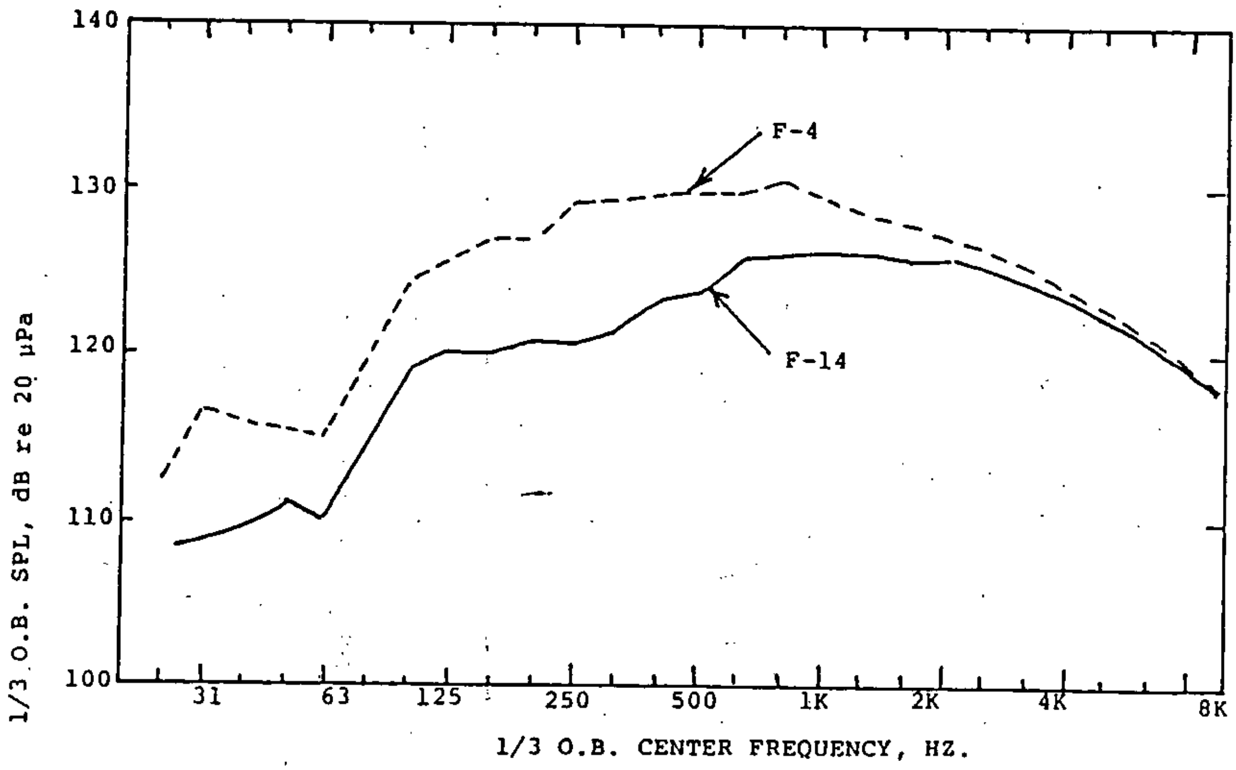

Figure 25
1/3-Octave Band Spectrum of the Interior Noise in the Miramar II Hush-House at Standard Microphone Position No. 3

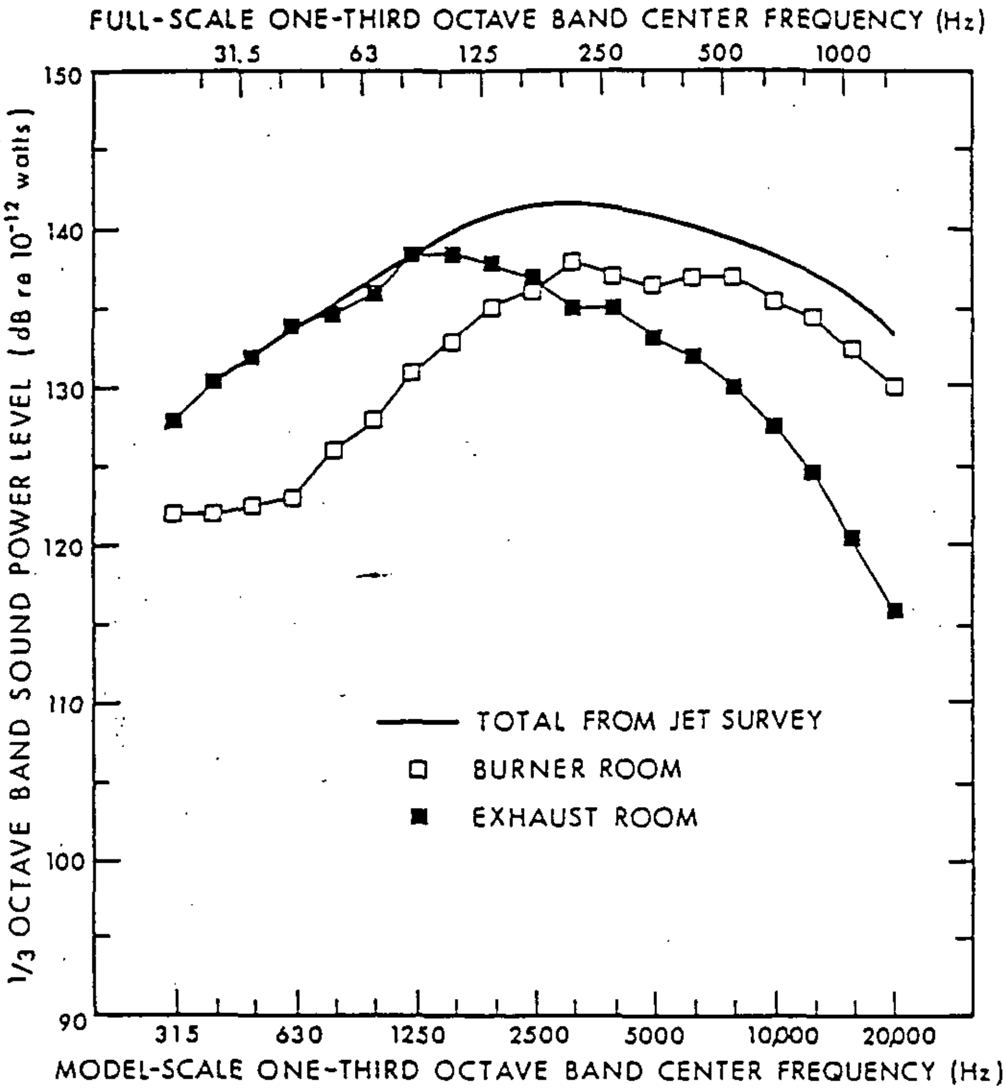

Figure 26
Split of Sound Power Between Enclosure (Burner Room) and Augmenter (Exhaust Room) Measured by Reference [3] Utilizing a 1/15-Scale Model: X_N = 10.5 in. 3300° R, λ = 2, D_A = 12.5 in., L_A = 72 in.

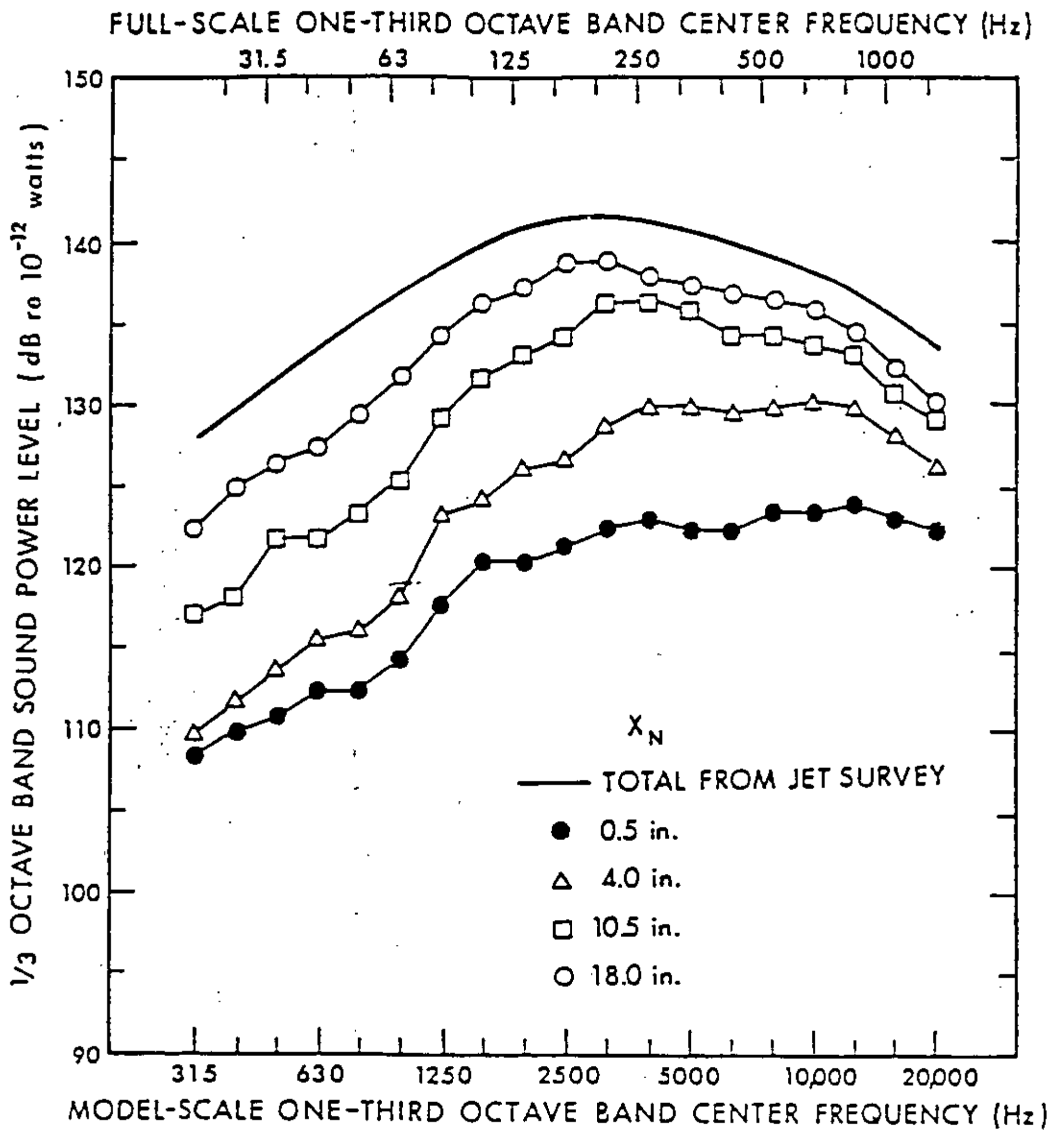

Figure 27
Effect of Axial Distance X_N on the Sound Power Radiated
into the Enclosure: 72-in. BBN
Augmenter, T_{TN} 3300°R, $\lambda_N = 2$

Section 12: EXTERNAL NOISE

12.1 Introduction. This section deals with the external noise of hush-house and jet engine test cells. Data reported in this section have either been obtained from full-scale facilities or from model-scale studies. The emphasis is placed on full-scale facilities. The far-field noise of ground runup facilities is of concern because, if not properly controlled, it can cause temporary hearing impairment, disturbance at nearby buildings within the base, disturbance to neighboring residences, and noncompliance with naval and community noise regulations.

12.2 Principal Paths of Noise Radiation. Figure 28 shows, in a schematic manner, the principal paths of noise radiated from a hush-house.

12.2.1 Path 1. Path 1 represents the attenuated jet noise which emerges from the exhaust end of the acoustically lined augmenter tube. The sound power radiated to the far field by the attenuated jet noise is a function of the:

a) sound power output of the engine(s);

b) axial distance of the engine exhaust plane from the augmenter inlet;

c) vertical, horizontal and angular positioning of the engine in relation to the augmenter axis;

d) geometry and acoustical treatment of the augmenter tube;

e) temperature and flow gradients across the augmenter cross-section created by the mixing of the hot exhaust jet with the surrounding cooling air;

f) acoustical characteristics of the lined 45° exit ramp.

12.2.2 Path 2. Path 2 represents the noise which is generated by the vortex shedding at the trailing edge of the exit ramp (or the trailing edge of baffles if the attenuation of the jet noise is accomplished with sound absorbing baffles located in the exhaust stack instead of the lined augmenter). This flow-generated noise is proportional from the 5th to the 6th power of the flow velocity at the trailing edge. Accordingly, the noise generated by this process is very sensitive to localized deviations of the exit velocity from its average value. Consequently, if the hot jet is not mixed sufficiently well with the surrounding cooling air to yield an even velocity distribution, then the flow-generated noise may contribute to the far-field noise. This is usually the case when the augmenter provides a high attenuation of the jet noise. Because of the directive nature of the flow noise, its contribution to the far-field noise is usually limited to position downstream of the exhaust.

12.2.3 Path 3. Path 3 represents the noise which radiates from the outside shell of the augmenter tube. Because the highest interior noise levels are in the vicinity of the entrance of the augmenter tube, this upstream portion of the exterior tube is usually the contributor to far-field noise.

12.2.4 Path 4. Path 4 represents the noise which escapes through the walls and roof of the building. The sound power escaping through this path is controlled by:

a) sound power output of the engine under test;

b) the axial distance between the engine exhaust and the plane of the augmenter intake opening;

c) horizontal and vertical positioning of the engine relative to the center line of the augmenter tube;

d) effectiveness of the sound absorbing treatment of the interior surfaces of the building;

e) sound transmission loss of the building walls, roof, and doors and windows in the exterior walls;

The above listed variables also control the interior noise in the building. Both the interior noise level and the sound power escaping through the building partitions increases strongly with increasing distance between engine exhaust and augmenter tube entrance.

12.2.5 Path 5. Path 5 represents the noise which escapes through large openings, such as the primary air intake. These large openings are necessary to bring in the large volume of air needed for the engine intake and for cooling. To control the noise escaping through these openings without excessive pressure drop (that would result in excessive cell depression), the sound attenuation must be accomplished by low-pressure-drop mufflers. Parallel baffle dissipative mufflers are the best to accomplish this and to provide an undistorted turbulence-free flow that is needed to avoid vortex generation especially in the front of the building upstream of the engine intakes.

12.2.6 Path 6. Path 6 represents the noise which escapes through the large front door of the building. Because of the shielding effect of the building, the noise radiated from the front door has practically no contribution to the noise at the far-field positions located in the downstream quadrant.

12.2.7 Source Receiver Paths. Source receiver paths which contribute to the far-field noise are summarized in Figure 29 in the form of a block diagram. This block diagram provides additional information for Figure 28. Figure 29 identifies the major noise source and the major paths through which part of the source noise reaches an observer located at a specific far-field position at 250-ft (76.2-m) radius circle (or any larger distance) centered at the engine exhaust. It illustrates that the noise at any observation point has contributions which arrive there via many different paths. Because directivity of radiation, the shielding by the building structure, and the source receiver distances are different for each receiver position, the prediction of the noise level at a specific receiver location is a difficult task. The task is even more complicated because the directivity and shielding effects for each particular source-path combination usually depends on frequency.

Due to the complexity of the problem, sufficiently accurate prediction of the far-field noise is possible only if carried out on the basis of appropriate scaling of measured noise data obtained during the field checkout of completed test cells and hush-houses of similar construction, whereby the scaling is aided by the results of systematic scale model studies and by theoretical considerations.

12.2.8 Effect of Geometry Change on Noise. The acoustical data presented in Sections 11 and 12, and in Acoustic Report on the 1/15-Scale Hot/Cold-Flow Model Tests of Forcing Cone Augmenter Pickup for Hush-Houses and Test Cells [17]; 1/15-Scale Model Testing of Dry-Cooled Jet Engine Noise Suppresors Using Hot Jet Simulating the TF-30-P-412 Fan Jet Engine [18]; Noise Levels of NAS Lemoore Cell #1 [20]; Letter Report on the Acoustical Performance Checkout of the NAS Dallas Jet Engine Test Cell [24]; and Noise Levels from the Operation of the J79-GE-80 Engine in the NAS Dallas, Texas, Air-Cooled Round Stepped Augmenter Test Cell [25]; and References [1, 3, 9, 21, 22, and 23], and Noise Levels of NARF, North Island Test Cell No. 20, R.E. Glass [19] can serve as a base for predicting exterior and interior noise of new facilities that have different geometry and utilize different engines than previously used. Based on the experiences that small changes in geometry or operating parameters sometimes can result in substantial changes in noise, scaling of data is not a simple matter.

12.3 External Noise of Full-Scale Test Facilities. The external noise of hush-house and jet engine test cells of the U. S. Navy is evaluated at seven standard microphone positions equally spaced (i.e., 30° apart) on a 250-ft (76.2-m) radius half-circle (experience shows that the polar plot is practically symmetrical around the axis of the facilities. Consequently, a 360° coverage is not necessarily centered at the engine exhaust. The first far-field microphone position (0°) is in the front and seventh (180°) behind the exhaust stack.

The A-weighted sound pressure level at these standard 250-ft positions is compiled in Table 6. This table includes far field noise data obtained for four hush-houses and three test cells. It contains 231 data points obtained for the A-4, A-6, F-4, F-14, F-18, and S-3 naval aircraft and for the J79-GE-8D, F-404, TF41-A2B, J57-P10, and TF30-P408 engines operating in military and maximum afterburner setting.

Figure 30 shows the 1/3-octave band spectrum of the far-field noise obtained at the Miramar No. 2 hush-house at front (0°) and aft (180°) location at 250 ft when the port engine of the F-4 aircraft was operating at max A/B. References [1, 9], and [20 to 25], and Noise Levels of the NARF Alameda Test Cell No. 15 [26], contain 1/3-octave band spectra obtained at all far-field positions for the test facilities for which A-weighted levels are listed in Table 6.

12.4 External Noise Studies Utilizing Scale Models. Most of the model studies undertaken dealt with the split of sound power between the enclosure and the augmenter entrance and with the sound-power-based attenuation of various augmenter configurations [3, 17].

One investigation [18] also dealt with the direct comparison of the sound pressure level at the scaled far-field microphone positions obtained for the bare model jet and those obtained at the same positions for the model exhaust system, respectively.

For Figure 31, the results of a model-scale investigation show how the axial distance of the jet exhaust from the augmenter entrance, X_N, influences the sound power that enters the augmenter. The larger the axial distance, the smaller is the sound power that enters the augmenter at mid and high frequencies. At low frequencies, where the noise source is within the augmenter, the axial distance has little influence on the sound jet power that enters the augmenter.

In Figure 32, the results of a model-scale investigation show how the particular position of a 12-in. (304.56 mm) long (15 ft (4.57 m) at full-scale) lined augmenter segment with a 60-in. (1523 mm) (75 ft (23 m) at full-scale) hard-walled augmenter influences the power-based insertion loss.

References [3, 17, and 18] contain results of scale-model acoustical studies for a variety of model-scale engines, exhaust system configurations, and specific acoustical treatments.

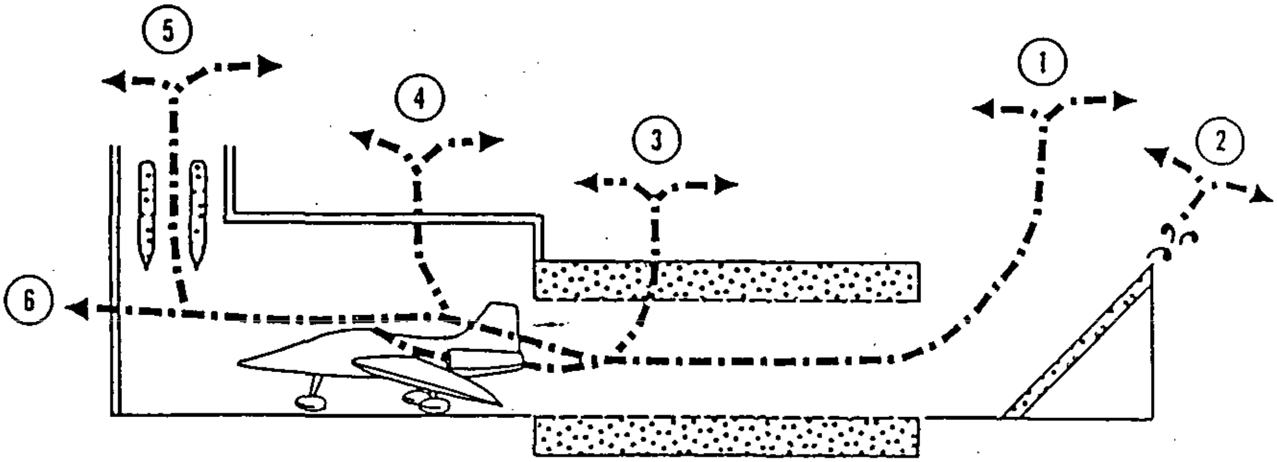

1. Attenuated Jet Noise
2. Flow-Generated Noise
3. Flanking through the Augmenter Tube Wall
4. Transmission through the Building Walls & Roof
5. Transmission through the Intake Muffler
6. Transmission through the Front Door.

Figure 28
Principal Paths of Noise Radiated from a Hush-House

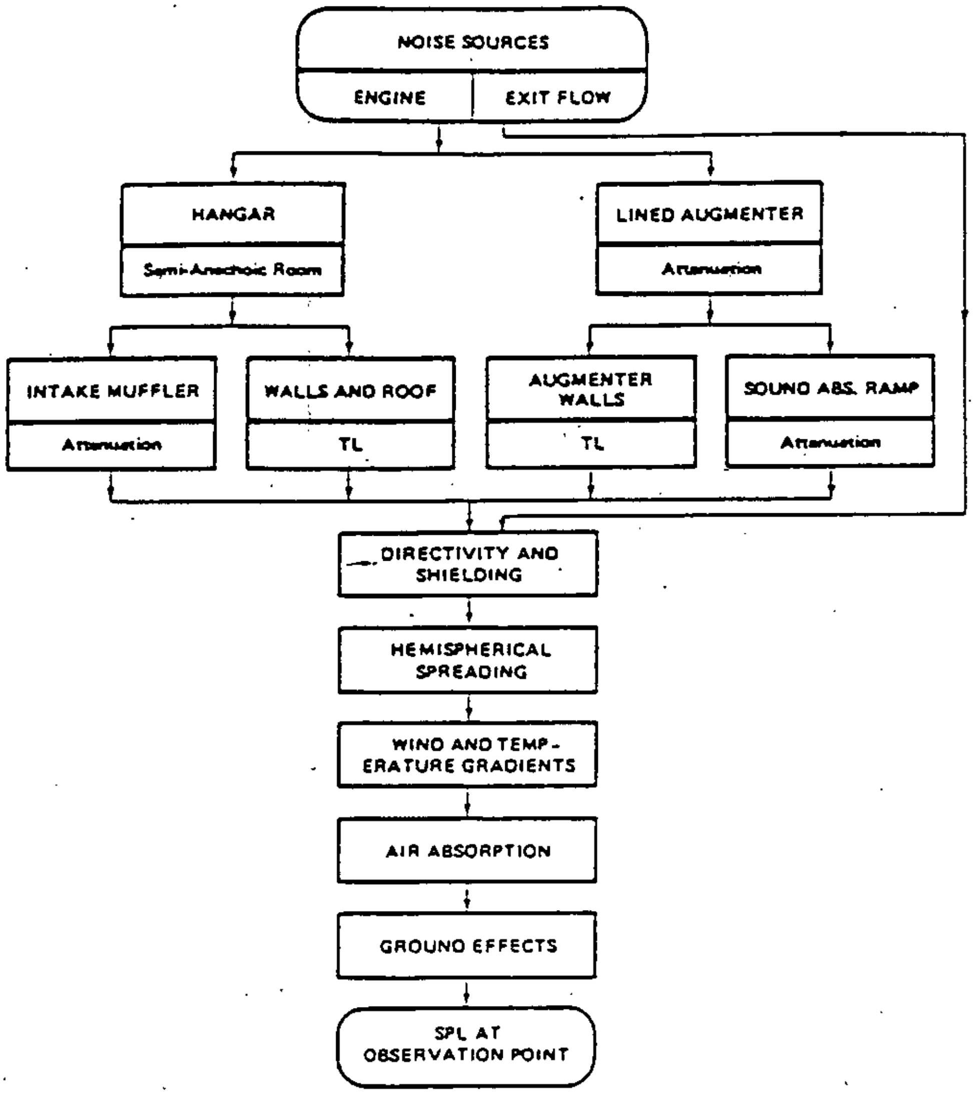

Figure 29
Source-receiver Paths for Exterior Noise in a Hush-House or Jet Engine Test Cell

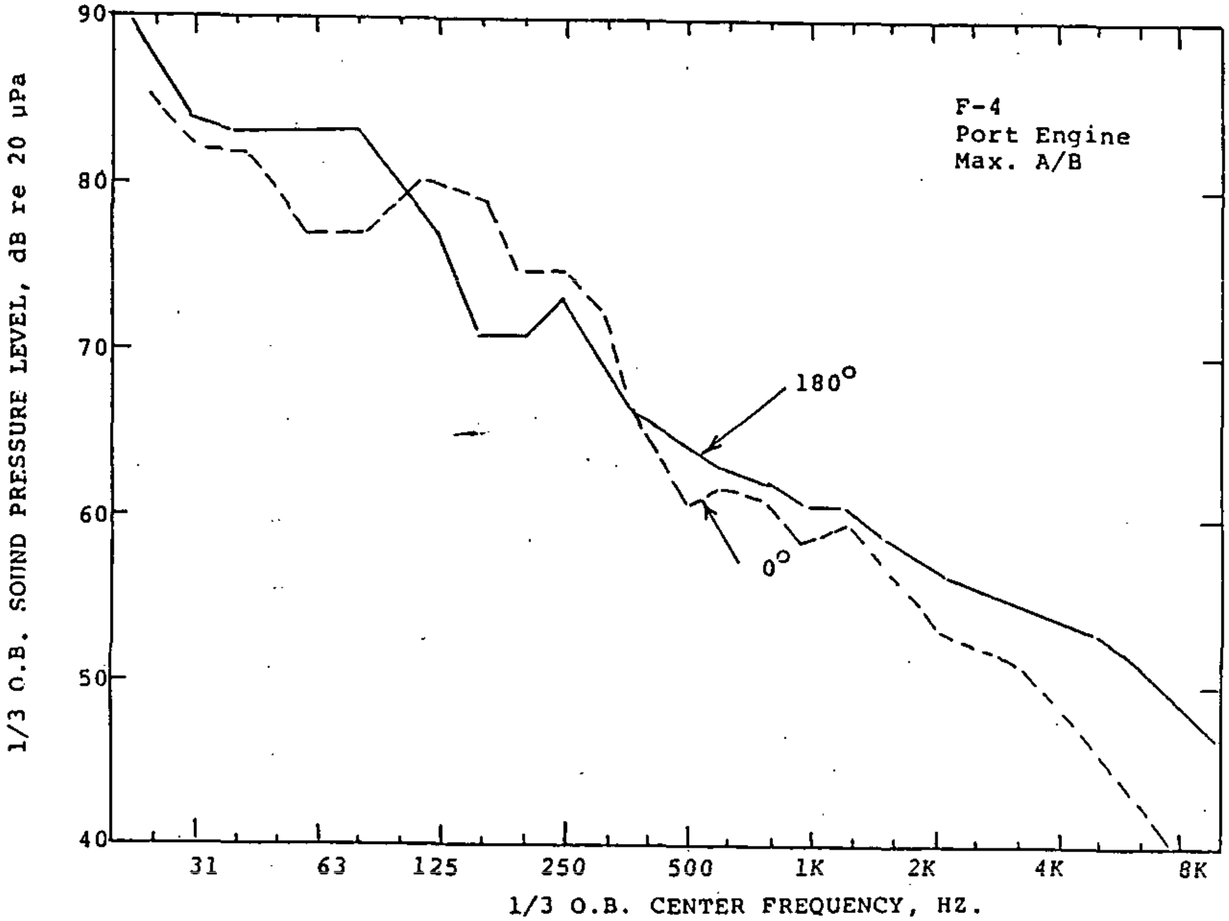

Figure 30
1/3-Octave Bank Spectrum of the Far-Field Noise
at 250 ft: Miramar II Hush-House

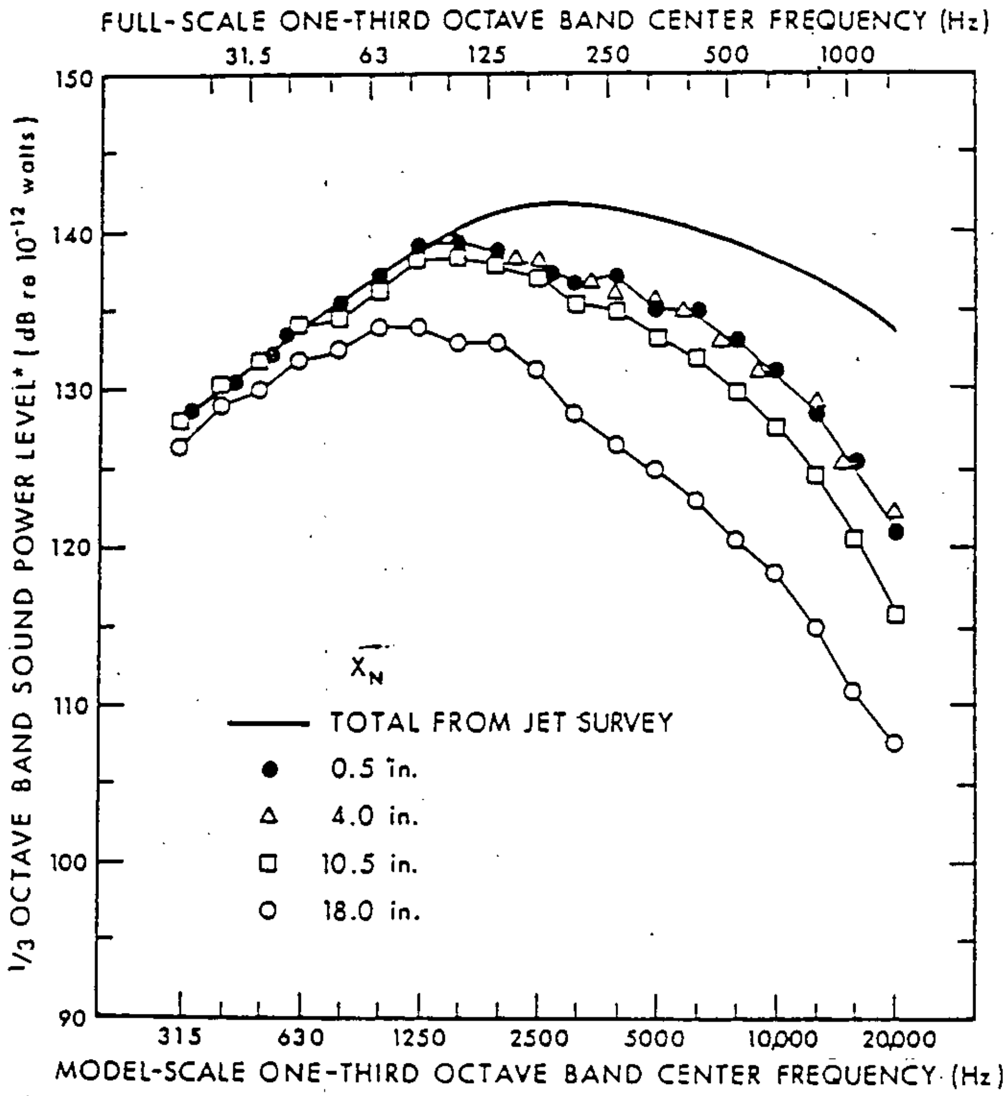

* At model scale only.

Figure 31
Effect of Axial Distance, X_N, on the Sound Power Radiated into the Augmenter; 3300°R, $\lambda_N = 2$, $D_A = 12.5$ in., $L_A = 72$ in.

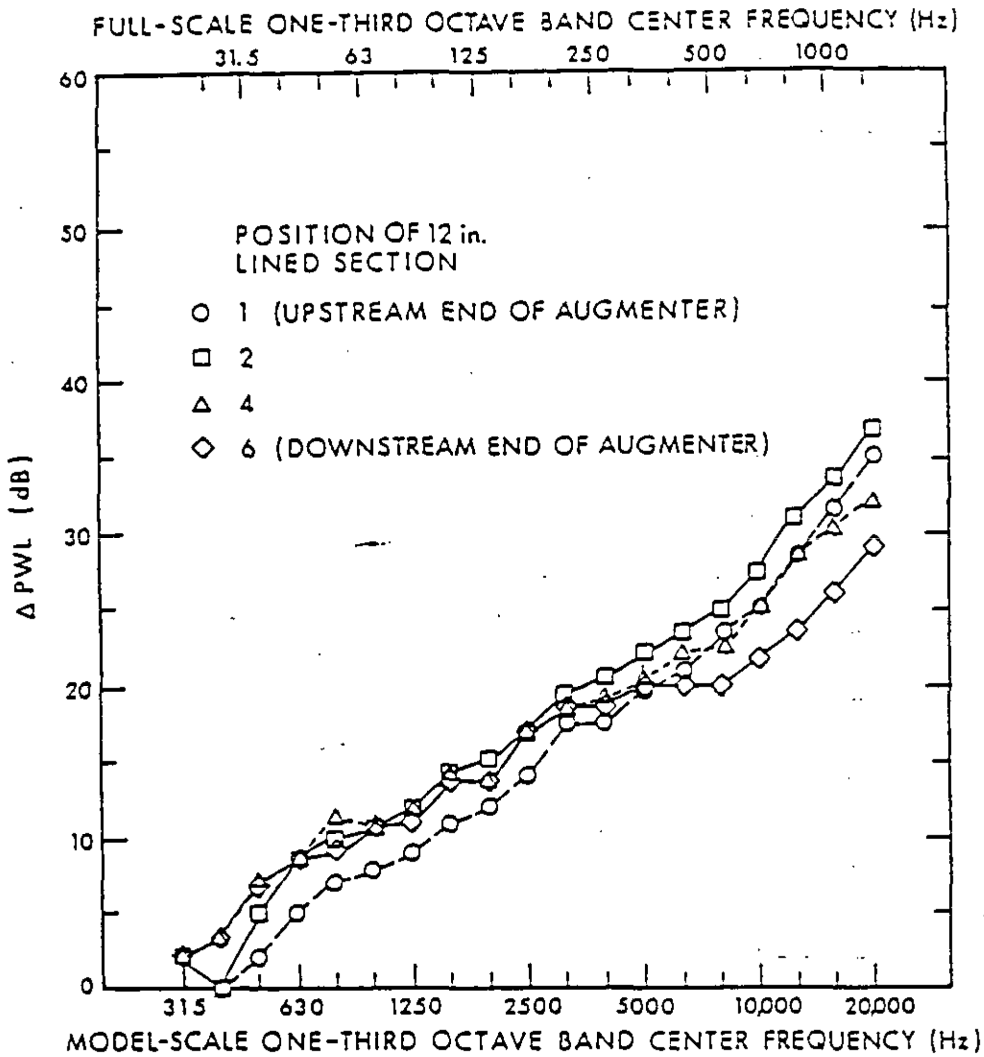

Figure 32
Power-based Insertion Loss, PWL, for 12-inch Section of Augmenter with BBN Liner at Various Positions in the 60-in. Hard-walled Augmenter with 45° Ramp; F-14 Position, T_{TN} = 3300° R, λ_N = 2, X_N = 4 in.

BIBLIOGRAPHY

The Use of a Hot Gas Ejector for Boundary Layer Control, Delco, R. V. and Wood, R.D., WADC TR52-128, April 1951.

REFERENCES

1. Aero-Thermal and Acoustical Data from the Postconstruction Checkout of the Miramar #2 El Toro Hush-House, Grunnet, J. L. and Ver, I. L., Navy Contract N62467-77-C-0614, April 1979.

2. Observation of Fluidynamic Performance of Miramar NAS F-4 Acoustical Enclosure and Recommendations for Improvement, Grunnet, J. L., (Revised) 21 June 1973.

3. Aerodynamic and Acoustic Tests of a 1/15 Scale Model Dry-Cooled Jet Aircraft Runup Noise Suppression System, Grunnet, J. L. and Ver, I. L., Navy Contract N62467-74-C-0490, October 1975. (Includes Checkout of Miramar #1 Hush-House).

4. NARF-NORVA Test Cells 13 and 14 Diagnostic Tests and Recommendations, Grunnet, J. L. (Aero-Dynamic) 1980.

5. Phase I Report - The Effect of Test Cell Exhaust System Design on Exhaust Plume Opacity - Analysis and Observations, Grunnet, J. L., Navy Contract N62467-80-C-0643.

6. A Study of Structural Failures in the Hush-Houses at NAS Miramar, Grunnet, J. L. and Getter, G., Navy Contract N62467-81-C-0582, July 1982.

7. Aerodynamic Measurements Made in the Marine A/E 32T-15 Engine Test Enclosure at Cherry Point (F-402-2), Relative to Pegasus Acceleration Lay and Subsequent Conclusions and Recommendations, Grunnet, J. L., Navy Contract N62467-81-C-0582 (Change P-0003), 1982.

8. Aero/Thermo Checkout of NAS Dallas Dry Cooled Jet Engine Test Cell, Grunnet, J. L., and Helm, N. C.,GGA Job 91000, January 1983.

9. Aero-Thermo and Acoustical Data from the Post-Construction Checkout of a Hush-House Located at NATC Patuxent River, Md., Grunnet, J. L., Helm, N. C., Ver, I. L., Navy Contract N62467-81-C-0582 (Change P00006) October 1983.

10. Aero and Thermodynamic Test of a 1/11.4 Scale Hush-House Augmenter Inlet, Idzorek, J. J., Conducted for the U. S. Navy by GGA

11. 1/15 Scale Cold Flow Model Tests of the Patuxent River Hush-House Configuration, Grunnet, J. L. and Berger, J. H., Navy Contract N6001-77-R-0182, December 1977.

12. Phase II and III Report--The Effect of Test Cell Exhaust System Design on Exhaust Plume Opacity-Model-Scale Plume Opacity Tests and Design to Procedures Minimize Opacity, Grunnet, J. L., and Phillips, W. H., Navy Contract N62467-80-C-0643.

13. 1/15-Scale Cold-Flow Model Tests of a Hush-House with Simulated AV-8 Aircraft Exhaust, Berger, J. H. and Leuck, J. L., "GGA Job Number 92900 April 1982.

14. 1/15-Scale Model Tests of a Forcing Cone Augmenter Pickup for Hush-Houses and Tests Cells, Buckley, T. F., and McDonald, T. J., Navy Contract N62467-81-C-0582, April 1983.

15. Holt Flow Model Tests of a 1/15 Scale Hush-House with Augmenter Flare and Forcing Cone Flow Pickups, Buckley, T. F., and McDonald, T. J., Navy Contract N62467-81-C-0582 (Change P-0005) October 1983.

16. Model Test and Full-Scale Checkout of Dry-Cooled Jet Runup Sound Suppressors, Grunnet, J L., and Ference, E., AIAA, J. Aircraft, October 1983, pp. 866-871.

17. Acoustic Report on the 1/15-Scale Hot/Cold-Flow Model tests of Forcing Cone Augmenter Pickup for Hush-Houses and Test Cells, Ver, I. L. and D. W. Anderson, BBN Letter Report submitted to FluiDyne Engineering Company, 16 June 1983.

18. 1/15 Scale Model Testing of Dry Cooled Jet Engine Noise Suppressors Using Hot Jet Simulating the TF-30-P-412 Fan Jet Engine, Morse, B. E. and G. E. Monge, U. S. Ocean System Center, San Diego CA (August 1980) U. S. Navy Contract Numbers N66001-78-C-2549 and N66001-80-C-2549.

19. Noise Levels of NARF, North Island Test Cell No. 20, Glass, R. E., NOSC TN 1284, September 1983.

20. Noise Levels of NAS Lemoore Cell #1, Glass, R. E., NOSC TN 1313, November 1983.

21. Experimental Evaluation of the NAS Miramar Hush-House, Sule, W. P. and E. T. Pulcher, NAEC-GSED-96.

22. Noise from F-18 and F-14 Aircraft Operating in Hush-House #2 at Naval Air Station Miramar, AESO Report No. 332-01-82, December 1982.

23. Noise Levels of the NAS Patuxent River, Maryland Hush-House, Glass, R. E., NOSC TN 1275, August 1983.

24. Letter Report on the Acoustical Performance Checkout of the NAS Dallas Jet Engine Test Cell, Ver., I. L., submitted to Gustav Getter Associates by Bolt Beranek and Newman, Inc. 25 February 1983.

25. Noise Levels from the Operation of the J79-GE-80 Engine in the NAS Dallas, Texas, Air-Cooled Round Stepped Augmenter Test Cell, Glass, R. E., NOSC TN 1246, February 1983.

26. Noise Levels of the NARF Alameda Test Cell No. 15, Glass, R. E., NOSC TN 1299, December 1983.

CUSTODIAN
NAVY - YD

PREPARING ACTIVITY
NAVY - YD

PROJECT NO
FACR - 0181

STANDARDIZATION DOCUMENT IMPROVEMENT PROPOSAL

(See Instructions – Reverse Side)

1. DOCUMENT NUMBER	2. DOCUMENT TITLE
MIL-HDBK-1197	AERO-ACOUSTICS TEST PROGRAMS

3a. NAME OF SUBMITTING ORGANIZATION

b. ADDRESS *(Street, City, State, ZIP Code)*

4. TYPE OF ORGANIZATION *(Mark one)*

- ☐ VENDOR
- ☐ USER
- ☐ MANUFACTURER
- ☐ OTHER *(Specify)*: ______
- ☐ EFD/PWO
- ☐ AE
- ☐ CONTRACTOR
- ☐ OICC/ROICC

5. PROBLEM AREAS

a. Paragraph Number and Wording:

b. Recommended Wording:

c. Reason/Rationale for Recommendation:

6. REMARKS

7a. NAME OF SUBMITTER *(Last, First, MI)* – Optional

b. WORK TELEPHONE NUMBER *(Include Area Code)* – Optional

c. MAILING ADDRESS *(Street, City, State, ZIP Code)* – Optional

8. DATE OF SUBMISSION *(YYMMDD)*

(TO DETACH THIS FORM, CUT ALONG THIS LINE)

DD FORM 1426, 82 MAR

PREVIOUS EDITION IS OBSOLETE.

NAVFAC Overprint